INSTITUTO SUPERIOR DE ENGENHARIA DO PORTO
MESTRADO EM ENERGIAS SUSTENTÁVEIS




Analysis of Forest Effects in Wind Farm Performance

José Daniel Rodriguez Mariscal
Junho de 2012

POLITÉCNICO
DO PORTO

Analysis of Forest Effects in Wind Farm Performance

José Daniel Rodríguez Mariscal

A thesis submitted in partial fulfilment for the requirements of the degree of
Master in Sustainable Energies

Instituto Superior de Engenharia do Porto (ISEP)
Mechanical Engineering Department

June, 2012

A report for Curricular Unit Internship of the 2nd year of Master of Sustainable Energies.

Student: José Daniel Rodríguez Mariscal, Nº 1111330, 1111330@isep.ipp.pt
Scientific supervisor: Doutor Carlos Silva Santos (CMI), CMI@isep.ipp.pt
Co-supervisor: Eng. Rui Faria Pereira (Megajoule Inovação), Doutor José Carlos Lopes da Costa (LOC)LOC@isep.ipp.pt

Company: Megajoule Inovação, S.A.
Address: TECMAIA - Rua Eng. Frederico Ulrich, 2650; 4470-605 Moreira da Maia
Company supervisor: Doutor Carlos Silva Santos, Eng. Rui Faria Pereira.

A mis padres y a mis abuelos.

Agradecimientos

Agradedezco a todos los que habéis hecho posible que este proyecto saliera adelante.

En primer lugar al Profesor Carlos Silva Santos y al Ingeniero Rui Faria Pereira por haber demostrado una enorme paciencia conmigo y haber conseguido introducirme en el mundo de la energía eólica. A todo el equipo de Megajoule por su acogida y por hacer de mi estancia una experiencia gratificante y enriquecedora.

Gracias al Instituto Superior de Engenharia do Porto y a la Universidad de Sevilla, así como a todos los que han hecho posible que programa Erasmus se lleve a cabo un año más.

Y por último, muchas gracias a Ana, a mis hermanos y a mis padres por haber logrado durante todo este tiempo la difícil tarea de soportarme.

Abstract

The objective of the thesis is to analyze the behaviour of the wind flow when it is passing beside the forest. To complete this analysis, a parametric study was done based upon generalized situations. Some abacus have been made, which are related to forest and wind characteristics.

The abacus were compared with a particular real case, namely Alexandrovo (Bulgaria), where it was concluded that the applicability of the abacus in projects with complex terrain is low and they must be used, from a quantitative point of view, for flat terrain, being h_c the most important parameter.

Keywords: Wind energy, Forests, Wind flow.

Resumo

O objetivo da tese é analisar o comportamento do fluxo do vento que passa pela floresta. Para realizar esta análise foi feito um estudo paramétrico com situações generalizadas, tendo-se construído ábacos que relacionam os parâmetros da floresta com as características de vento.

Em seguida, estes ábacos foram aplicados a um caso real, Alexandrovo (Bulgária), onde se constatou que a sua aplicabilidade é baixa em terreno complexo e que o seu uso, de um ponto de vista quantitativo, deverá ser restricto a terreno plano, sendo a altura da floresta o parâmetro de maior relevância.

Palavras-chave: Energia eólica, floresta, fluxos de vento.

Contents

List of Tables

List of Figures

Nomenclature

Upper-case Roman

SF	Shear factor.
TI	Turbulence intensity.
H_b	Bell height.
C_D	Drag coefficient.
F_i	Canopy drag force component.
S_ϵ	ϵ Equation canopy term.
S_κ	κ Equation canopy term.

Lower-case Roman

h_c	Height of canopy forest.
v_h	Horizontal velocity.
z	Cartesian vertical coordinate.
z_{agl}	Vertical coordinate above ground level.

Script Greek

α	Leaf foliage area per unit of volume.
θ_b	Bell slope.

Symbols

()'	Perturbation.

Abbreviations

a.g.l.	*Above ground level*
a.t.c.	*After canopy border*
a.s.l.	*Above sea level*
FT	Flat terrain.

$BT_{\pm 7^\circ \pm 14^\circ \pm 21^\circ}$	Bell terrain with different slope.
LAI	Leaf Area Index.
CFD	Computational Fluid Dynamics.
DNS	Direct Numerical Simulation.
RaNS	Reynolds averaged Navier-Stokes.
LES	Large Eddy Simulation.
ALX1	Mast ALX1, Gorna area.
ALX2	Mast ALX2, Rosina area.
ALX3	Mast ALX3, Alexandrovo area.
S3	SODAR S3, Alexandrovo area.
ABL	Atmospheric Boundary Layer.
A-WF	Alexandrovo-Wind Farm.
c.f.	Clockwise from.
MJ	MEGAJOULE.

Chapter 1

Introduction

1.1 Context the project

The wind energy development has caused the construction of new wind farms. The increased number of wind farms and the shortage of ideal sites have forced the industry to consider the possibility of installing wind farms in the vicinity of forests.

One of the problems of installing wind farms in these areas are the unknown characteristics of forests. In this thesis, the author has tried to produce tools to make such tasks easier.

In order that this objective is sucessful, a parametric study has been produced. The results of parametric study are compared with real situations to check behavioural standards.

This analysis aims to obtain a global qualitative vision. Due to lack of previous measurements of forests characteristics, only obtained on site wind measurements are to be used.

1.2 Motivation and objective

The principal motivation is the larg worldwide investment in wind energy. The fact that wind turbines are being sited in regions with mixed topography and forests, there is a need to develop quantitative understanding of the wind behaviour. There is a need for increased knowledge on the flow over trees and also in software tools that can properly address this problem.

1.3 Overview of Thesis

The Master Thesis was introduced in the first chapter.

The second chapter contains a short overview of the state of the art of wind flow over forests.

The third chapter presents the result of the parametric study, performed with the WINDIE^{TM} software for the following parameters: horizontal velocity, turbulence intensity and shear factor.

The fourth chapter compared the parametric study to a practice case study, Alexandrovo (Bulgaria).

The final chapter summarized the global conclusions for the Master Thesis.

Chapter 2

Literature review

2.1 Historical Background

The increasing population and consumption levels require more resources to sustain way of life. The demand for these resources affects, of course, power consumption, and therefore energy resources. Fossil fuels have been threatened, in addition to the problems caused by a massive use of those, pollution, greenhouse effect, etc.

For decades, there have been alternative approaches to electricity generation from renewable sources. This thesis focuses on wind energy, particularly in the vicinity of forests.

Currently, the general development and interest in sustainable energy, particularly eolic, has created some serious problems when we set up a wind farm on the terrain. The best locations are already occupied and it forced us to look for sites near to forests. Therefore, it urged us to do a comprehensive study of wind flow passing through forests.

This creates technical complications and modifications to the traditional methods of analysis for the behaviour of the wind flow. The point of view of this thesis is an analysis of the influence on the characteristic parameters after the wind flows through a forest area and vice versa. For example, at a defined distance from the forest, we would like to have a quantitative idea of its effects on the wind characteristics.

2.2 Wind Characteristics

Let us first define the most significant wind characteristics we are interested in.

2.2.1 Horizontal Velocity, $\mathbf{v}_h$

The horizontal wind velocity is defined as:

$$v_h = \sqrt{u^2 + v^2}, \tag{2.1}$$

where u and v are the velocity components for x and y directions respectively.

2.2.2 Turbulence Intensity, TI

The turbulence intensity is defined as:

$$TI = \frac{\sqrt{\frac{2k}{3}}}{v_h}, \tag{2.2}$$

where k is the turbulent kinetic energy.

However, for wind measurement datas, the turbulence intensity is obtained as:

$$TI = \frac{\sigma}{v_h}, \tag{2.3}$$

where σ is the standar desviation of the horizontal velocity.

2.2.3 Shear Factor, SF

The shear factor from simulation mesh nodes:

$$SF_k = \frac{ln\left(\frac{v_{h\,k+1}}{v_{h\,k-1}}\right)}{ln\left(\frac{z_{agl\,k+1}}{z_{agl\,k-1}}\right)}, \tag{2.4}$$

where k is the nodal index in the vertical direction.

2.3 Experiences in Wind Tunnel

During wind research the wind tunnel has been used to better understand the complex pattern of flow generated by a tree (a permeable, random shaped, elastic object).

In Meroney (1968), the author studied a models forest canopy to simulate the meteorological characteristics of typical living forests. From the correlation of the measurements made, plus additional ones, on living trees at Colorado State University, $C_D = [1.0, 0.3]$, the authors concluded that ''these measurements indicate that the flow is inertially dominated''.

Measurements were made on small specimens of Colorado spruce, juniper and pine trees, followed by a variety of plastic, metal and brush model trees.

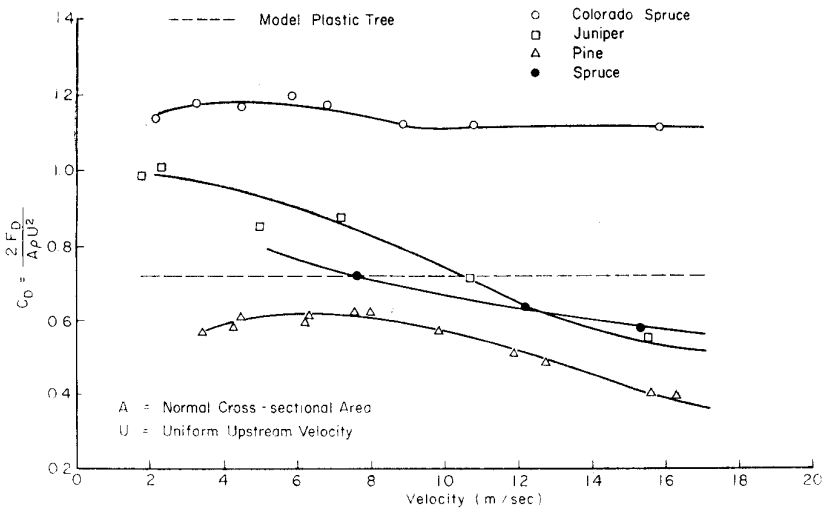

Figure 2.1: C_D of live and model trees - Meroney (1968)

It is apparent that the general behaviour of the wind flow has been simulated satisfactorily in the wind tunnel, as figures 2.2 and 2.3 are show.

In Neff and Meroney (1998), the study was divided in to a three phase researching programme to examine the wind flow over tree covered hills and ridges. The first phase of his work was a study of effects on wind flow due to individual trees, forest stands, and forest clearings. In the second phase, the measurements were made in wind tunnel of hill-top wind velocity profiles as a function of surface roughness, hill shape, and hill slope, figure 2.4. The last one, the autors examined the behavior of the wind flow over a scale model of a proposed wind energy site in the United States, New England region.

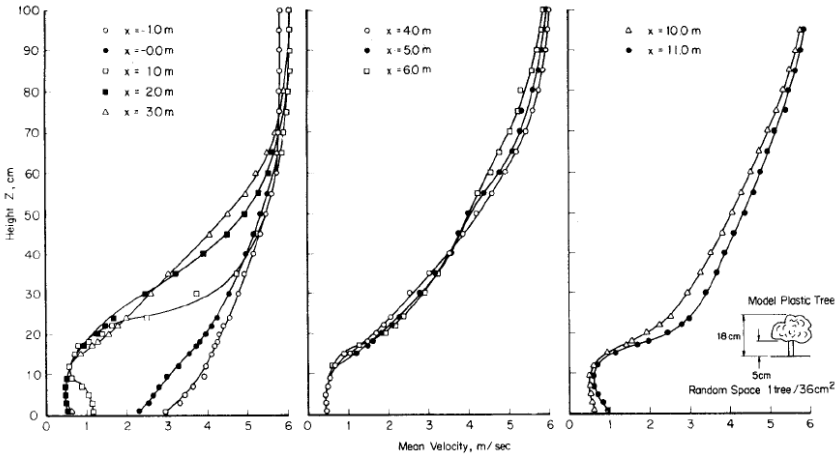

Figure 2.2: Velocity profiles in and above model forest canopy - Meroney (1968)

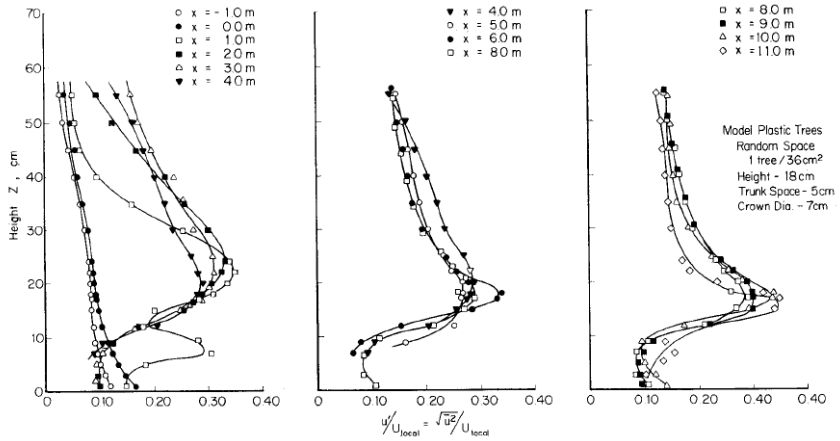

Figure 2.3: Logitudinal TI for model forest canopy - Meroney (1968)

In this test Neff and Meroney (1998), the effect of vegetation is generally limited to the region immediately above the terrain. Wind velicities near the ground increased substantially for even small clear cut operations at the crest. Turbulent intensities were primarily a function of the upwind forest height.

More recently, in Pedersen and Langreder (2007) an investigation was made to take on-site measured wind data from a number of sites inside of the forests and close to them around the globe with different kind of forests like pine, oak, olive trees, etc. Tha authors made some experiments in wind tunnel and the results were compared with wind measurements. The results are shown in following figure, 2.5, where TI at different measurement heights a.g.l. downstream from a forest edge can be seen.

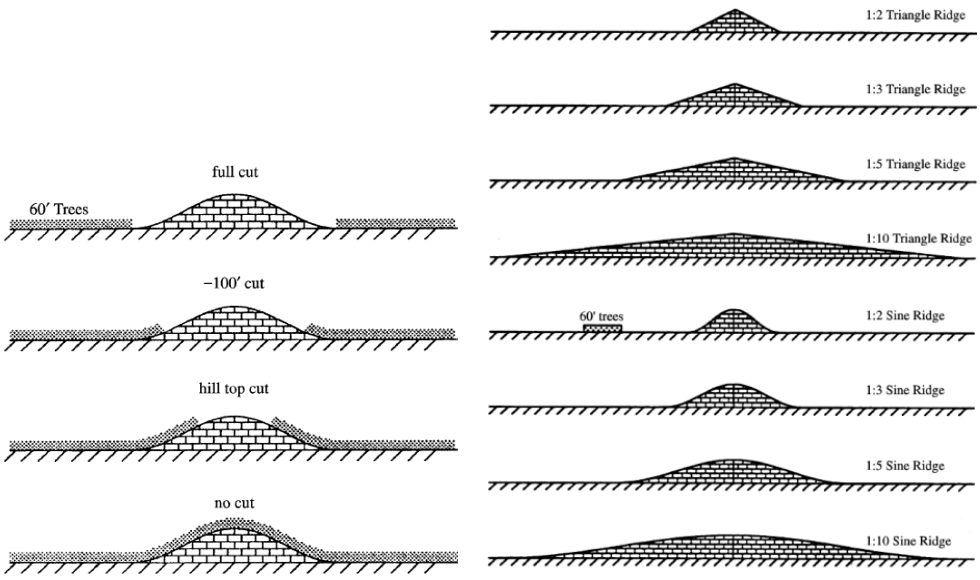

Figure 2.4: Model forest clearings on slope sinusoidal - Neff and Meroney (1998)

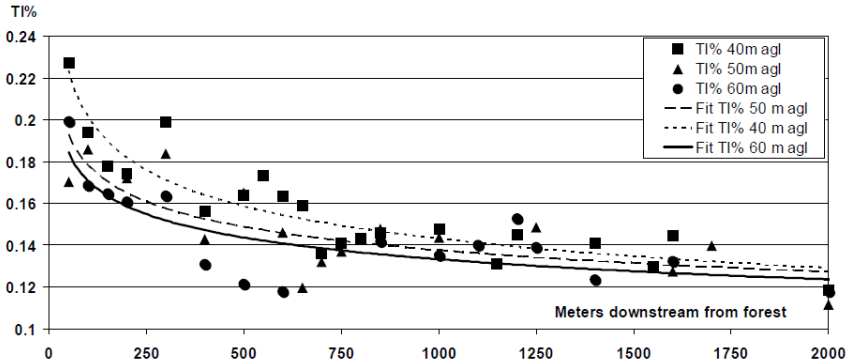

Figure 2.5: TI at measurement heights a.g.l. - Pedersen and Langreder (2007)

In this paper (Pedersen and Langreder (2007)), the authors observe that the presence of a forest has some significant effects on the flow field:

- Reduced wind speeds.
- Increased SF.
- Increased TI.

This distorted flow field has some negative effects regarding to loads and energy production for wind turbines downstream of a forest:

- It increases mechanical loads.
- It increases uncertainty in resource assessments.
- It increases uncertainty in turbine power curve.

In Rodrigo et al. (2007) a simple foam model that provides an effective simulation of the forest canopy flow has been modelled in a wind tunnel, following similar turbulence characteristics found in other wind tunnel and field tests, figure 2.6.

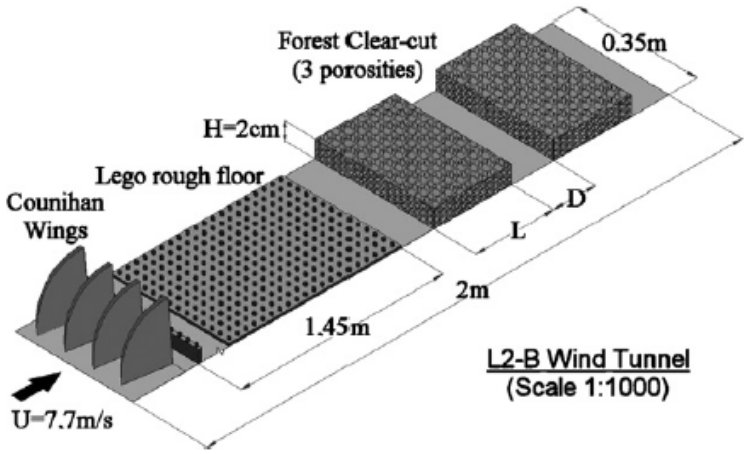

Figure 2.6: Sketch of the experimental set-up - Rodrigo et al. (2007)

The authors, Rodrigo et al. (2007), observed similar effects on the flow as already mentioned in Pedersen and Langreder (2007):

- The decrease of the energy content of the wind.
- The increase of TI.
- The increase of SF.
- The increase of extreme winds.
- The higher static and fatigue loading.
- The lower availability due to higher maintenance.

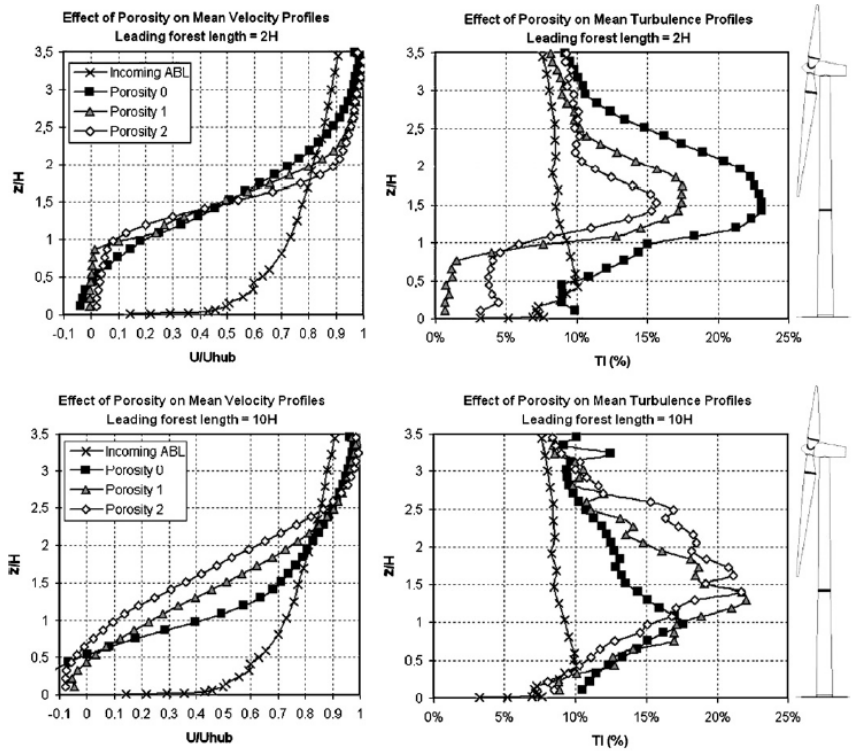

Figure 2.7: Profiles of mean velocity and TI in the middle of the cavity compared with incoming ABL profile - Rodrigo et al. (2007)

2.4 Wind measurements

An intimate knowledge of a site is essential for a lots of aspects of wind energy development, including site finding in the pre-development phase, resource assessment, wind flow modeling, turbine micrositing and wind farm energy yield optimization in the development phase, and power curve verification, wind-induced load measurements and even for insurance purposes in the operational phase.

To estimate the energy production of a wind farm, developers must first measure the wind on site. Data from the device for measuring wind velocity must be recorded for at least year to calculate an annually representative wind speed frequency distribution.

As wind turbines continue to grow in size, assembly masts of the cup anemometers necessarily become much higher, and more expensive.

This limitation has driven the commercialization of remote sensing tools for the wind energy industry. They are ground-based and can work over hundreds of meters, sufficient for the tallest turbines in the production or planned for it.

2.4.1 Description of CUP ANEMOMETERS

Cup anemometer is a device for measuring wind velocity, typically only horizontal wind velocities. It is composed of some hemispherical cups each one mounted on one end of a number of horizontal arms, which in turn are mounted at equal angles to each other about a vertical axis. The air flow past the cups in any horizontal direction turns the cups in a manner that it is proportional to the wind velocity.

Therefore, counting the turns of the cups during a set time period produces the average wind velocity for a wide range of speeds. Three-cup anemometers are currently used as the industry standard for wind resource assessment studies.

2.4.2 Description of SONIC ANEMOMETERS

Sonic anemometers provide quick and accurate measurements of the three dimensional wind velocity. These instruments are able to make measurements of wind velocity in the range $[0, 60]\, ms^{-1}$. Sonic anemometers operate measuring time necessary for a sound pulse to travel between a pair of transducers. This time depends on the distance between the transducers, sound velocity and wind velocity along the axis of the transducers.

The speed of sound in air depends on the temperature, pressure and contaminants in suspension such as dust and mist. In order to obtain the wind velocity between the trans-

ducers, each transducer alternates as transmitter and receiver so that the pulses trip to in both directions between them.

2.4.3 Description of SODARS

SODAR (SOund Detection And Ranging or 'acustics radar'), also written as sodar, is a meteorological instrument used as a wind profiler to measure the scattering of sound waves by atmospheric turbulence. SODAR systems are used to measure wind speed at various heights above the ground, and the thermodynamic structure of the lower layer of the atmosphere.

Sodar systems are like radar (radio detection and ranging) systems except that sound waves are used for detection rather than radio waves. These waves are reflected by moving aerosol particles in the flow, which allows the measurement of wind speeds by the Doppler effect.

2.4.4 Description of LIDARS

A LIDAR (LIght Detection And Ranging) is an active optical remote sensing instrument that transmits a laser beam (either as a continuous wave, or as a pulse) into the ABL (Atmospheric Boundary Layer) and measures the scattered radiation received back at the instrument.

LIDARs can use radiation in the ultraviolet, visible and infrared regions of the electromagnetic spectrum, and each of these will interact differently with the various physical processes within the atmosphere.

2.4.5 Comparation of SODARS vs CUP ANEMOMETERS

Advantages

The greatest advantage of SODAR is able to define wind profiles and measure wind velocities at high altitude, which would be prohibitively expensive to do with weather instruments mounted on towers, since the cost of these increases nonlinearly with height.

SODAR is an easily transportable device that is cheap to use in short-term campaigns. Meteorological towers may require special permits from the authorities; SODAR does not require such permits. SODAR does not disturb the flow of wind, unlike the meteorological towers, which do.

Disadvantages

SODAR system is not yet in widespread use in applications of wind energy production. The list of providers is limited. Being portable, they are vulnerable to theft and can be easily damaged. So it is not suitable to be used unattended for long-term measurement campaigns.

SODAR systems are also unreliable for turbulence measurements.

Although SODAR is portable, SODAR requires a stable platform. It can be especially useful in the context of offshore applications.

Operate in the audible frequencies can be a disadvantage in certain cases, it installed near residential area.

2.5 Numerical models

2.5.1 Introduction

The values for all study field have been obtained through the numerical models, they are based on some on site wind measurements.

In global wind energy study subject, two types of Wind Field Models dominate: linearised and CFD models. Linearised are very common because they require very limited computer power, they are fast and easy to use.

Linearised models are based on linearised solutions of the dynamic equations for boundary layer flow perturbed by terrain (simplified steady-state solutions of the Navier-Stokes equations). The governing momentum equations are linearised using scale analysis and assuming uniform rough surface and small slope.

Application of the theory to the wind energy sector led to the development of the most popular microscale modelling product: WAsP (in 1989).

Linearised models fail to predict and describe correctly the lee region where turbulent wake and separation develop. Further tests and applications proved the linearised theory to give reasonably good results on the upstream side and on the top of hills with $H/L = [0.3, 0.4]$, which corresponds to maximum inclinations of 22°.

2.5.2 Computational Fluid Dynamics - CFD

The equations of fluid mechanics - which have been known for over a century - are solvable for only a limited number of flows. The engineer has traditionally been forced to use other approaches. In the most common approach, simplications of the equation are used.

Flows and related phenomena can be described by partial differential (or integro-differential) equations, which cannot be solved analitically except in special cases. To obtain an approximate solution numerically, we have to use a discretization method which approximates the differential equations by a system of algebraic equations, which can then be resolved on a computer.

The mathematical model for incompresible flow, which is the approach used for the study of the atmospheric wind flow, is based on the resolution of the continuity and momentum equations (also known as Navier-Stokes equations) with integration of a turbulence model, in steady formulation. These equations express the physical principles of conservation of mass, momentum and energy.

CFD software solves the non-linear transport equations.

The differents approach to solve turbulent flows are:

It is possible to solve those equations using numerical techniques. It is called Direct Numerical Simulation - DNS. However, for complex geometry problems this involves a great deal of time and computer resources and frequently it is simply not feasible.

Alternative methods must be used in engineering studies, less demanding on computational resources, that enable us to obtain relevant solutions for the most of the flow geometries, such as the wind flow over topography.

Engineers are normally interested in knowing just a few quantitative properties of a turbulent flow. RaNS is the most interesting method for this objetive, it produce less information. However, some researchers were investigated turbulent flow above canopy forest using LES, e.g, Patton (1991) and Shaw and Shumann (1992).

In this work, Reynolds averaged Navier-Stokes (RaNS) method is used.

For our simulation we used WINDIE^{TM}, a computational fluid dynamics (CFD) code developed by a team of researchers from the Instituto Superior de Engenharia do Porto (ISEP, www.isep.ipp.pt) led by Prof. Fernando Aristides Castro.

WINDIE^{TM} is a non-linear model that solves the RaNS equations on terrain-following meshes. It is specially suited to capture complex phenomena such as flow separation, tur-

bulence induced by complex topography, thermal effects, large flow deviations and shear, as well as other flow features such as those induced by neighbouring forested areas.

A special formulation has been developed and used for modeling forest canopy. The most important modeling results are 3D wind field, vertical wind, wind inclination, wind shear and the turbulence.

For Forest Canopy Model, WINDIE^{TM} has one of the most advanced forest canopy models, extensively validated with real data, Lopes da Costa et al. (2006). It describes the vertical shape of the trees in terms of its leaf area density LAI and it has detailed interpolation techniques to model small or complex-shaped tree patches.

2.5.3 Mathematical models

.

To resolve the numerical problem adequately we need Navier-Stokes equations, mass and momentum conservation, furthermore, we need a turbulence model to solve the turbulent fields.

In our simulation, we used the following mathematical model. The mass conservation, momentum and $k-\varepsilon$ equations for a statistically steady turbulent flow in a boundary-fitted coordinate system are the following ones:

- From the mass conservation principle we obtain the continuity equation,

$$\frac{\partial \rho}{\partial t} + \frac{\partial(\rho u_i)}{\partial x_i} = 0, \tag{2.5}$$

- The momentum conservation principle (Newton's second law), when applied to a portion of fluid volume yields,

$$\frac{\partial(\rho u_i)}{\partial t} + \frac{(\rho u_j u_i)}{\partial x_j} = -\frac{\partial p}{\partial x_i} + \frac{\partial \tau_{ij}}{\partial x_j} + F_i, \tag{2.6}$$

where x_i are the Cartesian coordinates, u_i are the velocity components, ρ is the density (ρ=1.205 kgm^{-3}), t represents the time, p the fluid pressure and F_i is an external force that may act over the fluid.

As we considered that the wind flow is an incompressible flow, and that the air is a Newtonian fluid, there is a linear relation between the rate-of-strain tensor,

$$S_{ij} = \frac{1}{2}\left(\frac{\partial u_i}{\partial x_j} + \frac{\partial u_j}{\partial x_i}\right), \tag{2.7}$$

$$\tau_{ij} = 2\mu S_{ij}, \tag{2.8}$$

where μ is the dynamic molecular viscosity of air (μ=1.85e-5Nsm^{-2}).

The $k-\varepsilon$ equations without average notation, for RaNS methods:

$$\rho\frac{\partial k}{\partial t} + \rho\frac{\partial u_i k}{\partial x_j} = \frac{\partial}{\partial x_j}\left[\left(\mu + \frac{\mu_t}{\sigma_k}\right)\frac{k}{x_j}\right] + \mathcal{P}_k - \rho\varepsilon + S_k, \tag{2.9}$$

$$\rho\frac{\partial \varepsilon}{\partial t} + \rho\frac{\partial u_i \varepsilon}{\partial x_j} = \frac{\partial}{\partial x_j}\left[\left(\mu + \frac{\mu_t}{\sigma_\varepsilon}\right)\frac{\varepsilon}{x_j}\right] + \frac{\varepsilon}{k}(C_{\varepsilon 1}\mathcal{P}_k - C_{\varepsilon 1}\rho\varepsilon) + S_\varepsilon, \tag{2.10}$$

where ε and k are two scalars, k stands for the turbulent kinetic energy and ε the dissipation rate for turbulent kinetic energy; μ_t is the turbulent viscosity; $\mathcal{P}_{k,\varepsilon}$ are production terms and $S_{k,\varepsilon}$ are dissipation terms.

	$C_{\varepsilon 1}$	$C_{\varepsilon 2}$	C_μ	σ_k	σ_ε
Standard	1.44	1.92	0.090	1.0	1.30
Atmospheric flow	1.44	1.92	0.033	1.0	1.84

Table 2.1: $k-\varepsilon$ constants for standard and atmosferic flows

The "standard" engineering constants have been used for numerous types of flows. However, for atmospheric flows $C_\mu = 0.033$ is preferred to 0.09 so that μ_t matches its atmospheric surface layer value.

2.5.4 Canopy models

In this section, we will adjust the momentum and $k-\varepsilon$ equations, of the previous subsection, to include canopy forest coefficients.

The canopy presence is represented in the RaNS momentum equations as a drag force, thought to reproduce the momentum dissipation that the trees and its foliage should produce in the wind flow.

The term F_i represents an external force over the fluid, that in our case, will be the drag force induced by the presence of the forest canopy, consists of the sum, of pressure and viscous forces due to the vegetation.

$$F_i = -\rho a(z) C_D |U| \bar{U}_i, \tag{2.11}$$

where $|U|$ is the local mean velocity modulus, $a(z)$ (in $m^2 m^{-3}$) is the leaf foliage area per unit of volume. It can vary appreciably with z, especially for forested systems and C_D is the canopy drag coefficient, this coefficient value varies between 0.1 and 0.3 for most of the vegetation, Katul et al. (2004), in our simualtion, we used $C_D = 0.2$.

The term F_i is negative and that sign represents the momentum loss (aerodynamic drag) due to the foliage which must be accounted for inside an extended vertical region of height equal to the tree height.

The effects of the canopy on the turbulence, through mechanisms of turbulence production and destruction due to the canopy foliage, are also accounted for by the additional source/sink terms, S_k and S_ε, in the transport equations of k and ε.

$$S_k = \rho C_z \left(\beta_p |U|^3 - \beta_d |U| k \right), \tag{2.12}$$

$$S_\varepsilon = \rho C_z \left(\frac{\varepsilon}{k} C_{4\varepsilon} \beta_p |U|^3 - C_{5\varepsilon} \beta_d |U| \varepsilon \right), \tag{2.13}$$

where $C_z = C_D a(z)$ and $C_{4\varepsilon}$, $C_{5\varepsilon}$, β_p and β_d are the forest canopy model constants.

In table 2.2, the different configurations for various canopy models are shown.

The canopy model implemented in this work is that of Lopes da Costa et al. (2006).

Kinds of canopy forest

The presence of plant canopy in the surrounding terrain of a wind farm is an important issue in the modelling of the flow behaviour.

The next table summarizes the key aerodynamic and morphological attributes for some forest canopies. Some characteristics have been obtained from Katul et al. (2004) and Kaimal and Finnigan (1994).

Author	β_p	β_d	$C_{4\varepsilon}$	$C_{5\varepsilon 2}$
Svensson and Häggkvist (1990) and Lopes da Costa et al. (2006)	1.0	0.0	1.95	0.0
Green (1992)	1.0	4.0	1.5	1.5
Liu (1998)	1.0	4.0	1.5	0.6
Sanz (2003) and Katul et al. (2004)	1.0	5.1	0.9	0.9

Table 2.2: Set of constants found in the different canopy forest models

Property	Jack pine stand	Scots pine stand	Loblolly pine stand	Hardwood pine stand	Moga forest	Urriaga forest	Bordeaux forest	Spruce stand	Aspen stand
h_c (m)	15	20	16	22	12	20	13.5	10	10
LAI	2.0	2.6	3.8	5.0	1.0	4.0	3.0	4.0	10.0
$\bar{a}(m^2/m^3)$	0.13	0.13	0.24	0.25	-	-	-	-	-
C_d	0.2	0.2	0.2	0.15	0.2	0.2	0.2	0.2	0.2
α (a_{max})	0.2537	0.2474	0.4519	0.4325	0.1586	0.3806	0.4229	0.7611	1.9029
$\bar{a'}(m^2/m^3)$	0.1333	0.13	0.2375	0.2273	0.0833	0.2	0.222	0.4	1

Table 2.3: Forest kinds set

Figures 2.8, depict the forest characteristics of table 2.3 according to the following equation:

$$a(z) = a_{max}\left(\frac{h_c - z_{a_{max}}}{h - z}\right)^n exp\left(n\left(1 - \left(\frac{h_c - z_{a_{max}}}{h - z}\right)\right)\right), \tag{2.14}$$

where $z_{a_{max}}$ is the height a.g.l. where the maximum value of the leaf are density, a_{max} is the maximum value of the leaf area density, $n = 6$ for $z < z_{a_{max}}$ and $n = 0.5$ for $z > z_{a_{max}}$.

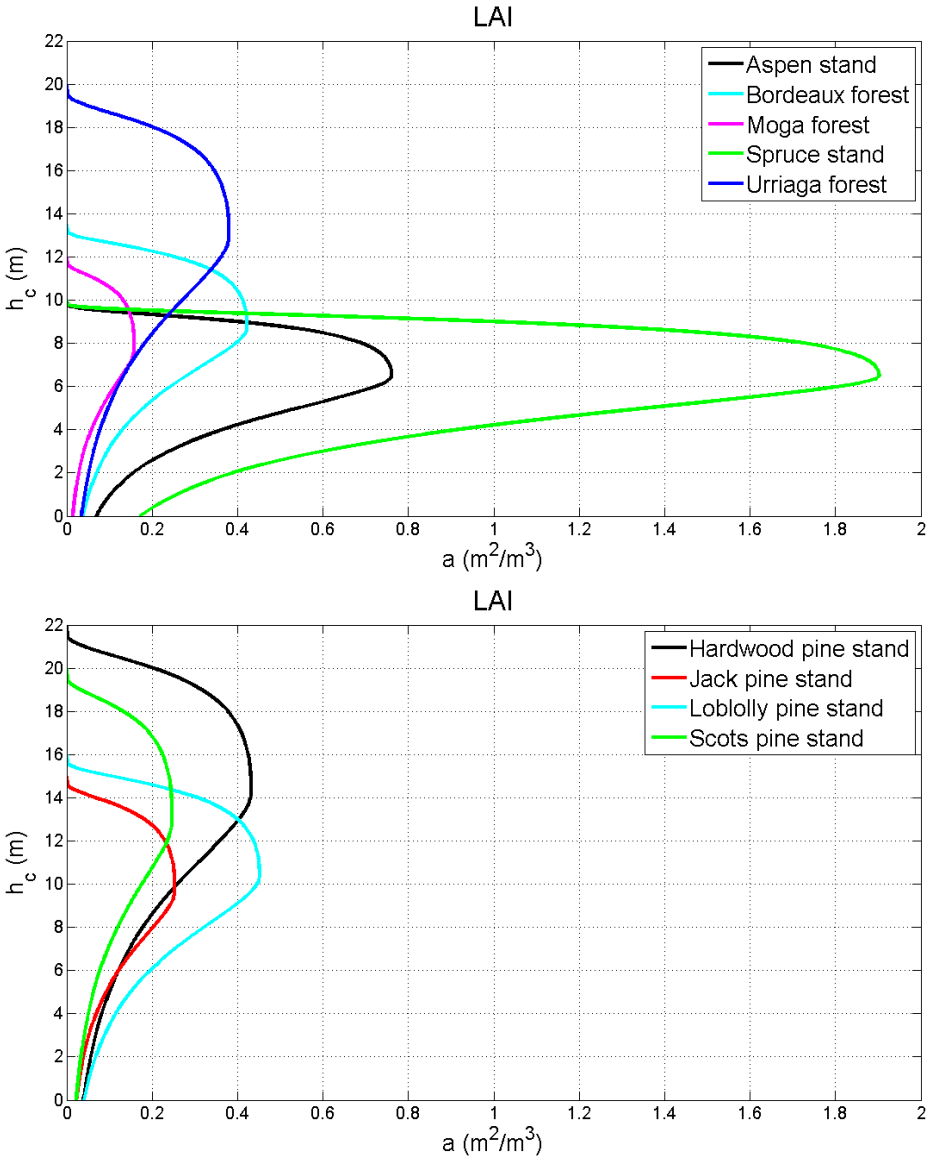

Figure 2.8: LAI for the different forest canopies

2.6 Conclusion

The main objective for this chapter was to know the state of the art related to wind behaviour, in particular v_h, TI and SF.

The chapter is the base for the parametric study and to optimize the use of forest canopy models.

Chapter 3

Parametric Study

3.1 Overview of parametric analysis

The objective of the parametric study is to determine the performance of the wind flow when passing through the forest canopy, so that, when forest features are unknown, an aproximate h_c and α can be estimated.

In order to understand the behaviour of the wind, we opted for a multi-parametric analysis with different topographical and forest canopy configurations. These have been simulated in software WINDIE^{TM}, with the goal of extracting behavioural patterns of the wind flow in terms of v_h and TI as SF.

In order to reach the maximum range of possible situations that can appear in practical studies and thus establish relationships as general as possible, we opted the following configurations:

- First, using MATLAB®, a flat topography with the area 50 km x 50 km and relative roughness of 0.03 was created.
- Secondly, a plain topography with constant slope of $\pm 7°$, $\pm 14°$and $\pm 21°$, was empoyed but convergence was difficult without altering the boundary conditions at the top of the domain.
- Finally, and in order to study the effect of forests on positive and negative slopes, a topography with a cosine bell was employed.

In terms of the position of the forests, within the topography, a band was introduced transversely to the wind flow, with 3 km width for flat terrain and 1 km for bell topography, either on the positive or negative bell slope.

There were six canopy forests combinations for the parametric study. They can be classified in two groups according to their common characteristics:

- Group 1 for observing the evolution of wind flow as a function of h_c (α=const.).
- Group 2 as a function of α (h_c=const.).

The different forest canopies are shown into next table 3.1.

Group	Name	$h(m)$	α	C_D
1st ($\alpha = const.$)	canopy no.1	5	0.2	0.1
	canopy no.2	10	0.2	0.1
	canopy no.3	20	0.2	0.1
2nd ($h = const.$)	canopy no.4	10	0.1	0.1
	canopy no.2*	10	0.2	0.1
	canopy no.5	10	0.4	0.1
	canopy no.6	10	0.6	0.1

Table 3.1: Forest kinds set.

* canopy no.2 is included in 1st and 2nd groups.

3.2 Flat terrain

In this section, the behaviour of wind flow over flat terrain is analysed.

For the simulation of the flat terrain topography was defined in MATLAB®, with the dimensions of 50 km x 50 km x 4.5 km. Our study area for WINDIE™ was 2000 m x 8500 m (fetch=1500 m; canopy=3000 m; downstream=4000 m). The relative roughness already mentioned above (apart from the canopy zone) is $z_0 = 0.03$.

Measuring distribution points are represented the majority of parametrical analysis for flat terrain on the figure 3.1.

The mesh distribution which has been simulated by WINDIE™, in the XY and XZ planes is shown above on the figure 3.2.

In WINDIE™ the results of v_h, TI and SF are calculated at all grid points, and, a posteriori, by post-processing tools or with software TECPLOT®.

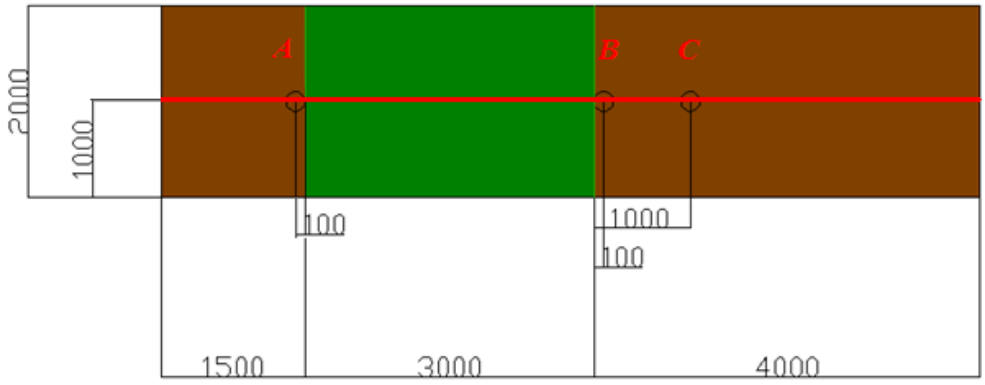

Figure 3.1: Canopy forest distribution on flat terrain

Direction	N	COF(x,y,z)	Δ
i (x)	122	70	8500
j (y)	32	70	2000
k (z)	30	$h_c/10$	4500

Table 3.2: Mesh features for flat terrain

The quantities of v_h, TI and SF are compared at the centre line of the study area for flat configuration. Besides, the v_h, TI and SF for different height a.g.l. [40, 85, 100 and 130] m have been compared, non-dimensionalised by the magnitude at 100 m a.g.l., i.e., the ratios $v_h/v_{h_{100\,m}}$, $TI/TI_{100\,m}$ and $SF/SF_{100\,m}$ are represented.

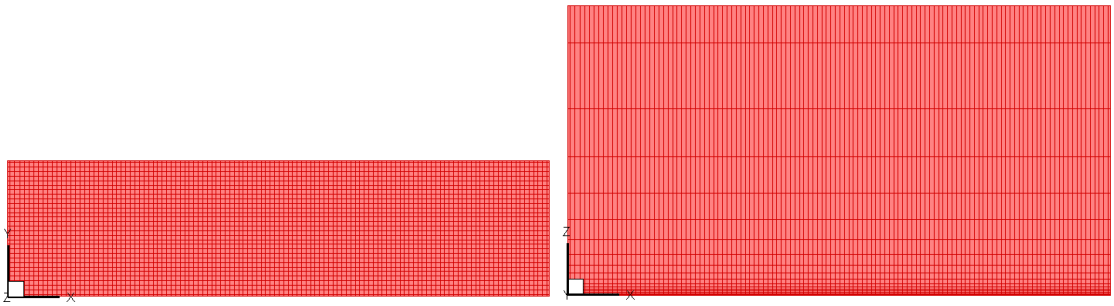

Figure 3.2: Grid distribution in plane XY and XZ for flat terrain

3.2.1 Effects of forest canopy height, h_c

Influence on v_h

The values of v_h are directly connected with h_c. Highest decreases in v_h are produced for high values of the h_c. Figure 3.4 shows that behaviour.

When the wind passes through the forest, v_h decrease, as it has been obtained by Lopes da Costa et al. (2006) and Raupach et al. (1996).

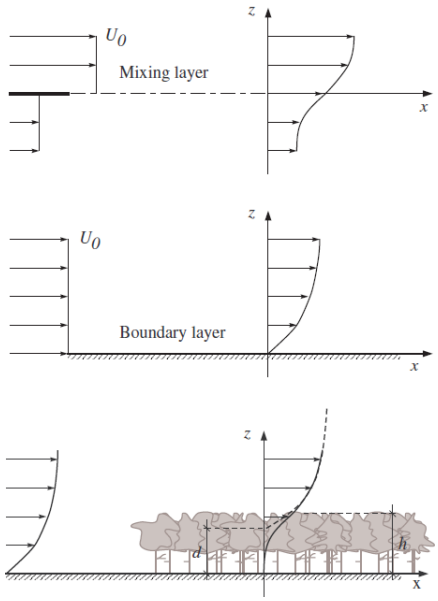

Figure 3.3: Displacement of boundary layer profile and mixing layer analogy

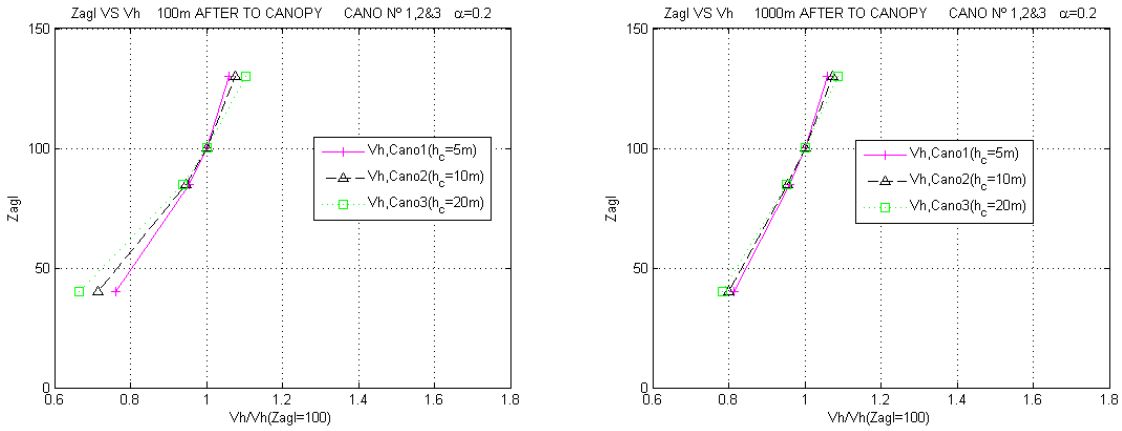

Figure 3.4: The v_h for group 1 at 100 m and 1000 m a.t.c., for flat terrain.

In figure 3.4, for a 100 m of distance from the forest border there is a difference of 10% in v_h for h_c= 5 m and h_c= 20 m 40 meters a.g.l.

This difference almost disappears at a 1000 m a.t.c., where it is reduce to 3%. For 40 meters a.g.l. however, the effects of the h_c in v_h are still seen.

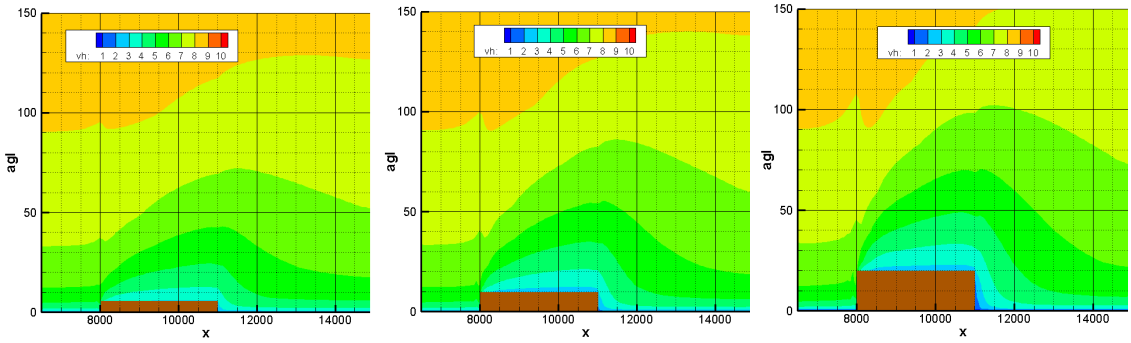

Figure 3.5: v_h for group 1 for flat terrain. From left to right: h_c = 5 m, 10 m and 20 m

Influence on TI

For heights a.g.l. lower than 80 meters, the increase of TI, caused by increasing h_c, is less noticeable. Therefore, for lower h_c, it takes longer to reach the regime that exists before the encounter beetwen the forest canopy and the wind flow (the gradient is lower). In others words, the TI decreases quicker with greater h_c.

At 100 m a.t.c., the values of TI for h_c = 5 m and h_c = 20 m are 60 % and 76 % higher than the TI at 100 m a.g.l., respectively. This can be observed in figure 3.6. It is observed that for a height from 40 m a.g.l., to 1000 m a.t.c., the values are similar for all values of h_c, 25 % higher than the TI to 100 m a.g.l..

This means that for the same distance (from 100 m to 1000 m a.t.c.) the TI drops: 33 % for h_c = 5 m and 52 % for h_c = 20 m, with respect to TI at 100 m a.g.l.

Obviously, the absolute magnitudes are greater for larger h_c, however the foregoing is reflected in increasing verticality of TI profiles to greater heights. This can also be observed in the contour maps of Figure 3.7, obtained by alicing the 3D flow field at the centre line.

Adding also what is shown in figures 3.6 and 3.7, to 1000 m a.t.c., the difference between the TI for different h_c are smaller.

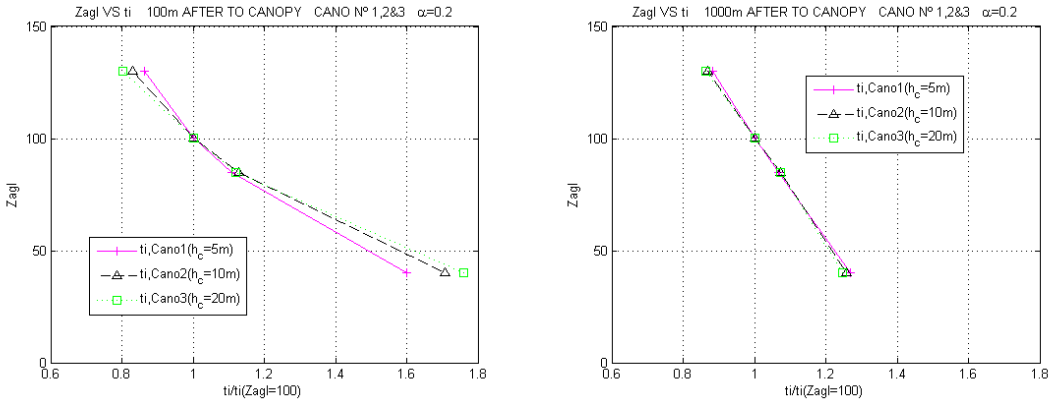

Figure 3.6: TI for group 1 at 100 m and 1000 m a.t.c., for flat terrain.

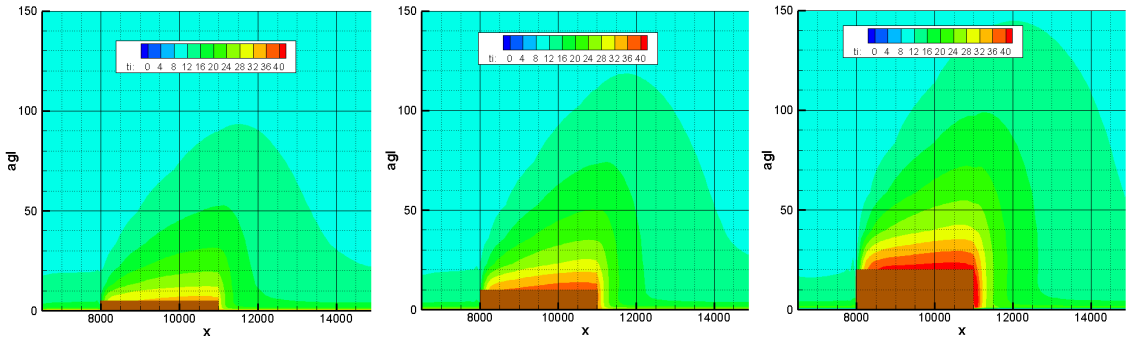

Figure 3.7: TI for group 1 for flat terrain. From left to right: $h_c = 5\,\text{m}$, 10 m and 20 m

Influence on SF

The SF takes higher values for higher h_c (the disturbance is greater). As this quantity is directly related to v_h profiles, they predictably have a similar behaviour.

However, for the analyses of variation h_c, with $\alpha = 0.2$, the values of the SF are within the range of operation of the wind turbine [0,0.2] from 4000 m in the most unfavorable case($h_c = 20\,\text{m}$) and approximately 2000 m in the best case ($h_c = 5\,\text{m}$). As it can be seen in figure 3.9.

We can therefore conclude that, according to the model, the forest has a sustaining effect on SF, which extends by several kilometers in flat terrain.

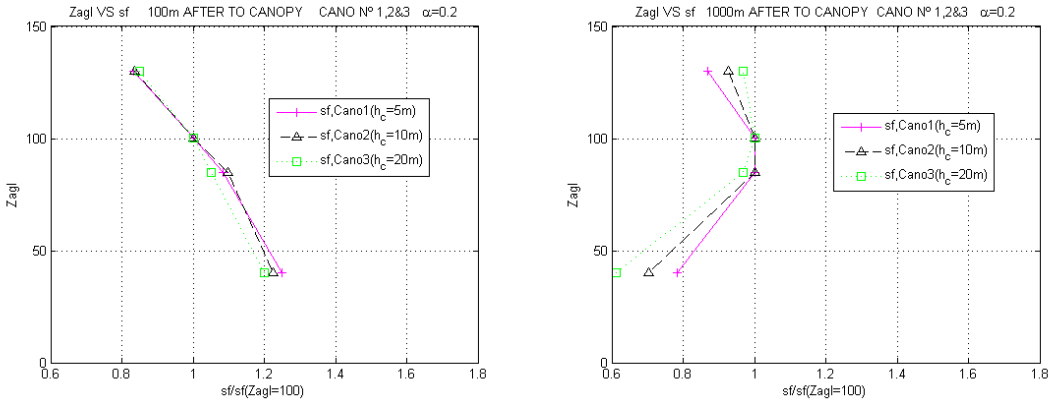

Figure 3.8: SF for group 1 at 100 m and 1000 m a.t.c., for flat terrain.

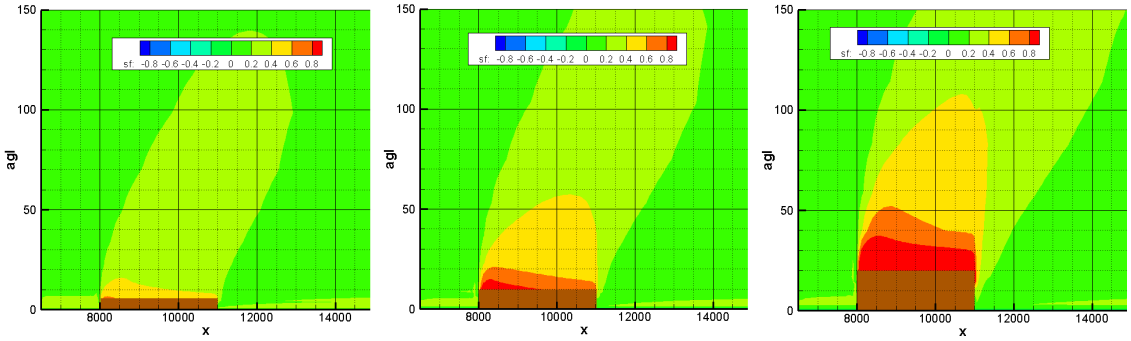

Figure 3.9: SF for group 1 for flat terrain. From left to right: $h_c = 5\,\text{m}$, 10 m and 20 m

3.2.2 Effects of leaf area idex, α

Influence on v_h, TI and SF

The differences in the values v_h, TI and SF, for different α and constant $h_c = 10\,\text{m}$ at 1000 m a.t.c., are negligible, with the exception of the value of $\alpha = 0.1$ where that the effects of disturbance are slightly lower, as shown in figure 3.10.

The effects of α, for close distances to the end of the forest and for low heights a.g.l., can be observed. However there is not influence of the α on the distance and working height of the turbines.

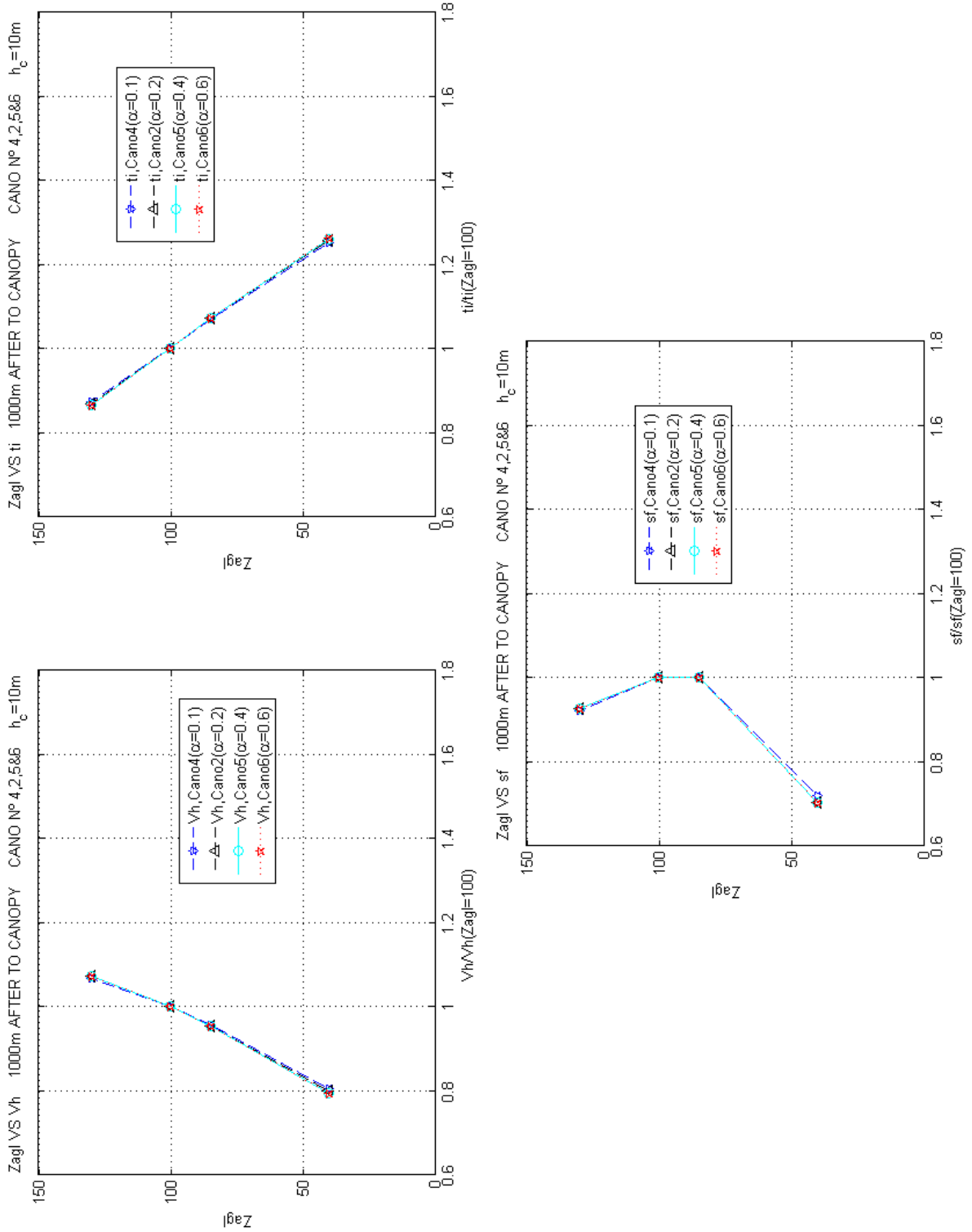

Figure 3.10: v_h, TI and SF for group no.2 to 1000 m a.t.c., for different α.

3.2.3 Quantitative conclusions for flat terrain.

This subsection, a guide from a practical point of view (of applicability) is tackled, obtaining conclusions of mathematical order. The algebraic relations (polynomials) between wind flow parameters and forest canopy characteristics give rise to the possible construction of an abacus.

The little influence of the effect of α is an important conclusion for the abacus construction, it was therefore removed as a variable, and a value of $\alpha = 0.2$ was fixed in this analysis.

The following input variables: x, z_{agl}, v_h, TI and SF, and the output variable is the h_c have been considered.

In line with the previous paragraph, the following figures, 3.11, show the decrease of v_h, the increase of TI and the increase of SF, for growing h_c and for various distances a.t.c..

Finally, the abacuses are created summarizing this information and establishing relationships at z_{agl}, between wind flow parameters measured on site and h_c.

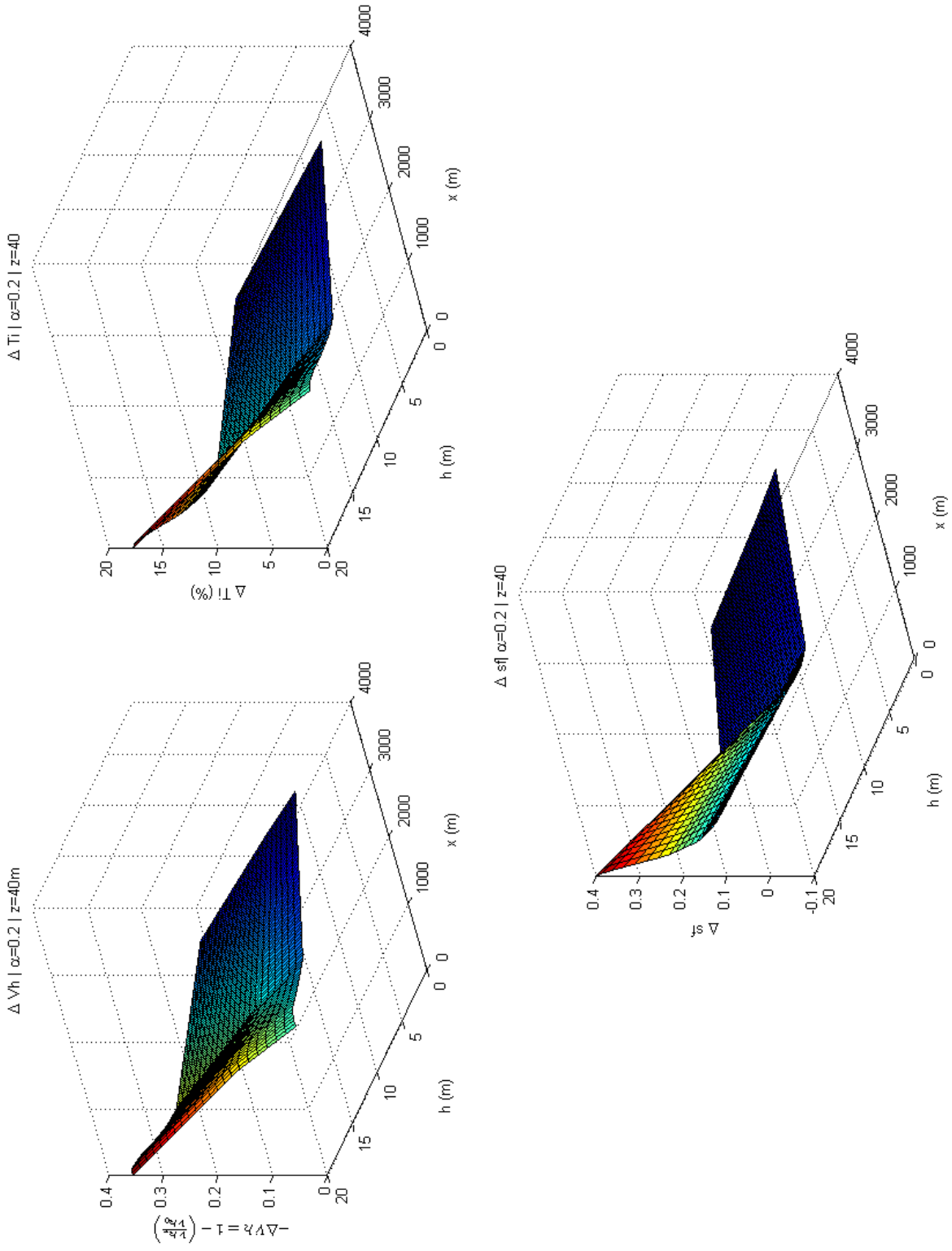

Figure 3.11: v_h, TI and SF, depending on h_c, FT, at z_{agl}=40m

.

3.3 Bell Terrain

In this section, the behaviour of wind flow over bell terrain is analysed. In one case the forest is presented on the positive slopes, while in the other it is placed on the negative inclination.

For the simulation on bell terrain, a topography in MATLAB® was defined with a surface of 50 km x 50 km, the relative roughness (apart from canopy zone) is $z_0 = 0.03$.

Direction	N	COF(x,y,z)	Δ
i (x)	180	70	10000
j (y)	30	70	6000
k (z)	50	$h_c/10$	5000

Table 3.3: Mesh features for bell terrain

Default parameters for the parametric study with bell terrain are shown:

Up-slope, Θ_b [+07°, +14°, +21°].

Fetch to end of canopy = 3000 m; canopy = 1000 m; downstream = 10000 m.

Down-slope, Θ_b [-07°, -14°, -21°].

Fetch to end of canopy = 4000 m; canopy = 1000 m; downstream = 9000 m.

For each slope (±07°, ±14°, ±21°) six simulations were performed with the characteristics listed in the table 3.4. It follows that the BT parametric study comprised 36 (6x6) simulations in total.

Name	$h(m)$	α	C_D
canopy no.1	5	0.2	0.1
canopy no.2	10	0.2	0.1
canopy no.3	20	0.2	0.1
canopy no.4	10	0.1	0.1
canopy no.5	10	0.4	0.1
canopy no.6	10	0.6	0.1

Table 3.4: Simulation features for bell terrain

The forest distributions are represented in figure 3.12 for the positive and the negative slopes of bell, along with the places where measurements points are located on which the parametric study is based.

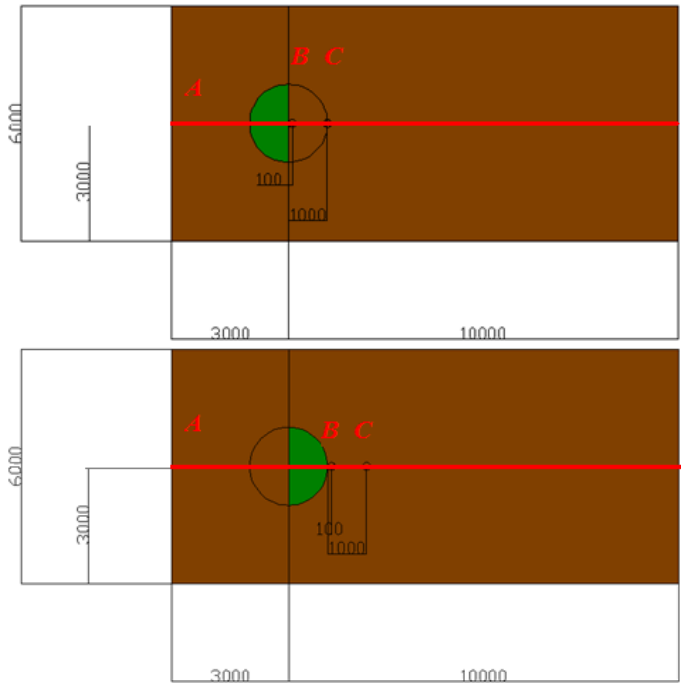

Figure 3.12: Canopy forest distribution on bell terrain

The mesh distribution which has been simulated by WINDIE^{TM}, in the XY and XZ planes is shown in figure 3.13.

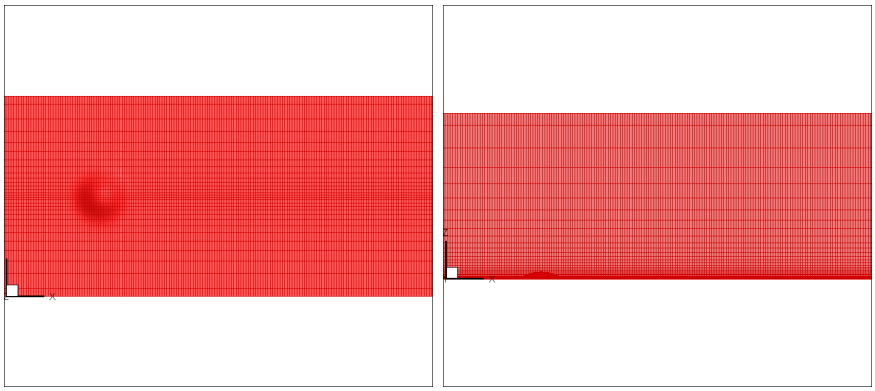

Figure 3.13: Grid distribution in plane XY and XZ for bell terrain

The values of the v_h, TI and SF are compared at middle of the study area at points B and C. Also the v_h, TI and SF for different height a.g.l. [40, 85, 100 and 130] m, non-dimensionalised by the magnitude at 100 meters, have been compared, i.e., the ratio: $v_h/v_{h_{100\,m}}$, $TI/TI_{100\,m}$ and $SF/SF_{100\,m}$ are represented.

At point $(9000\,, 25000)$ the centre of the bell (with $1\,km$ radius) is located, defined by,

$$z = H_b \cos\left(\frac{\pi r}{2}\right)^2, \tag{3.1}$$

By varying H_b we obtained the following slopes, table 3.5:

Name	Θ_b	H_b (m)
Bell no1	$\pm 7°$	85.6
Bell no2	$\pm 14°$	160.5
Bell no3	$\pm 21°$	240.8

Table 3.5: Bell defined and their features.

For different binomial combinations between the characteristics of the forest canopy (h_c and α) and terrain features (H_b and Θ_b) many different effects on wind flow can occur.

3.3.1 Positive bell terrain

In the following subsection, the h_c and α effects on the wind flow are observed on bell terrain with forest on the positive slope.

Effects of forest canopy height, h_c

For $\Theta_b = +07°$, there is an influence h_c in the behaviour of the v_h, TI and SF. The v_h is inversely proportional but the TI and SF are directly proportional to h_c.

For $\Theta_b = +21°$, at $x = 1000\,$m a.t.c., there is a high degree of disorder and discordant behaviour for different heights. This suggests that the high terrain slope is causing flow separation and that the topography effects dominate over forest effects.

For $\Theta_b = +14°$, the evolution of v_h, TI and SF are halfway between slopes of $\Theta_b = +07°$ and $\Theta_b = +21°$ happen.

For $\Theta_b = +07°$, $\Theta_b = +14°$ and $\Theta_b = +21°$ at $100\,$m a.t.c., when varying the h_c (group 1) for a specific Θ_b, there are not significative differences, as shown in Figures 3.14, 3.15 and 3.16.

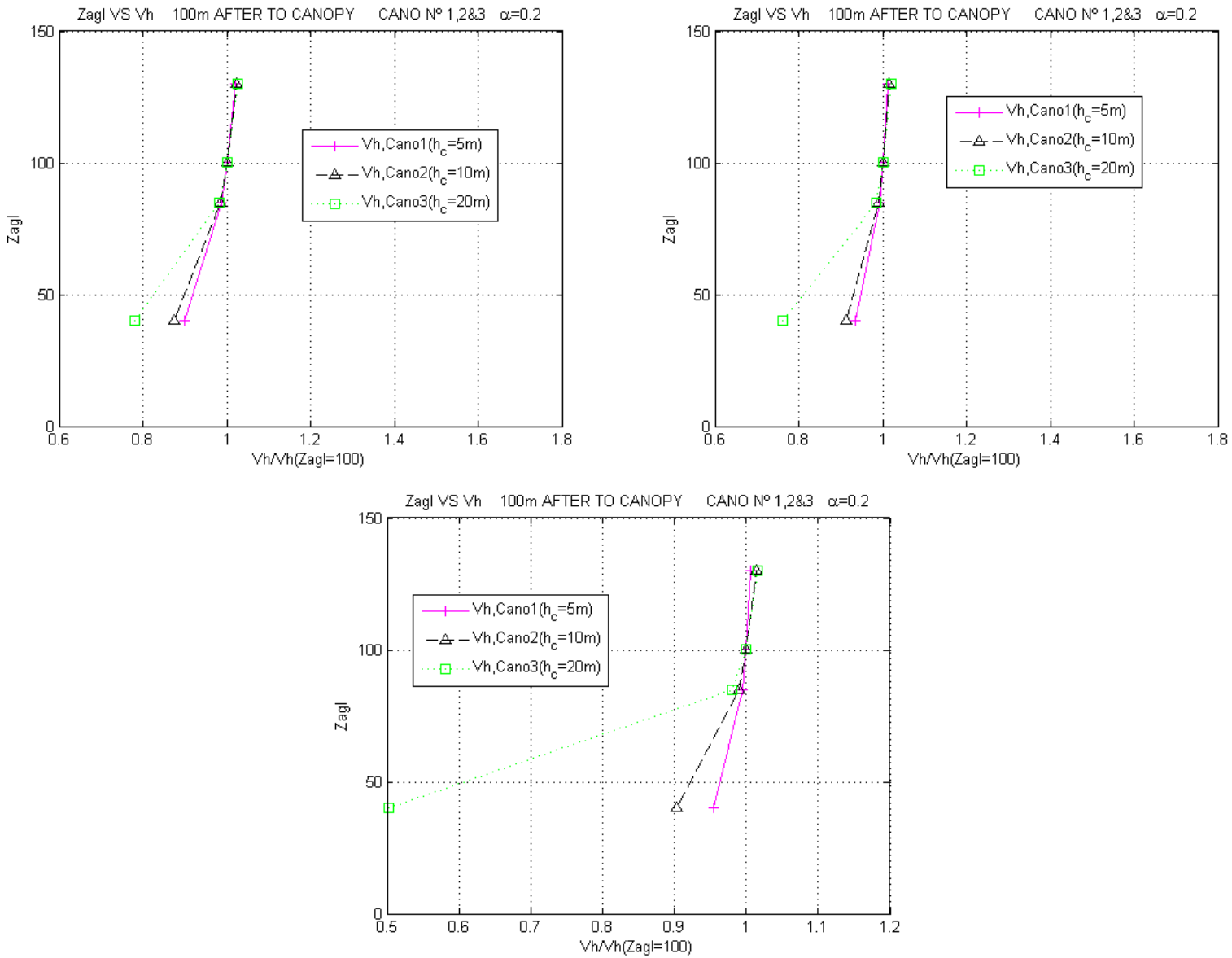

Figure 3.14: v_h at x =100 m a.t.c., for Θ_b= +07°, +14°and +21°, clockwise for (c.f.) top left

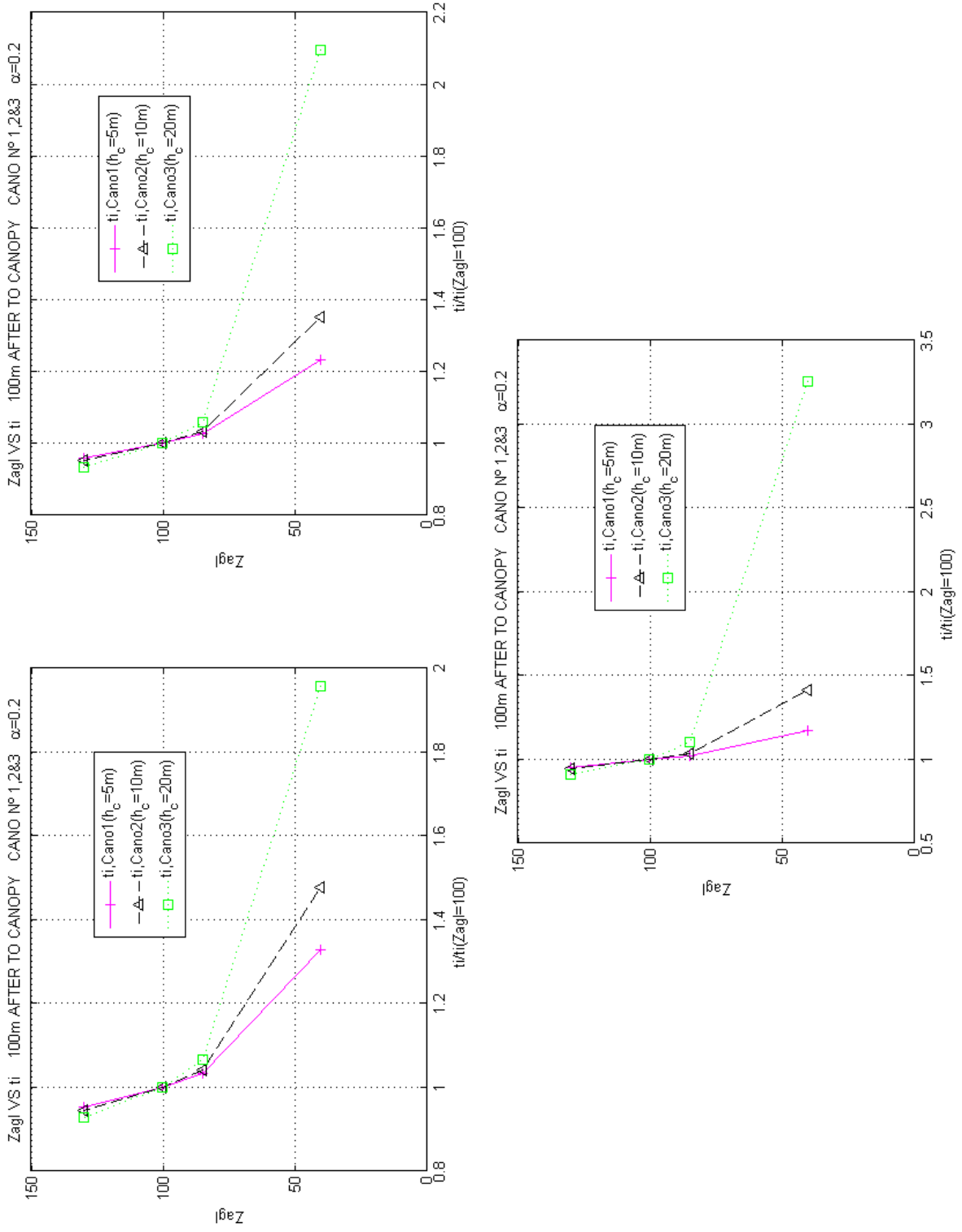

Figure 3.15: TI at x =100 m a.t.c., for Θ_b= +07°, +14°and +21°, c.f. top left

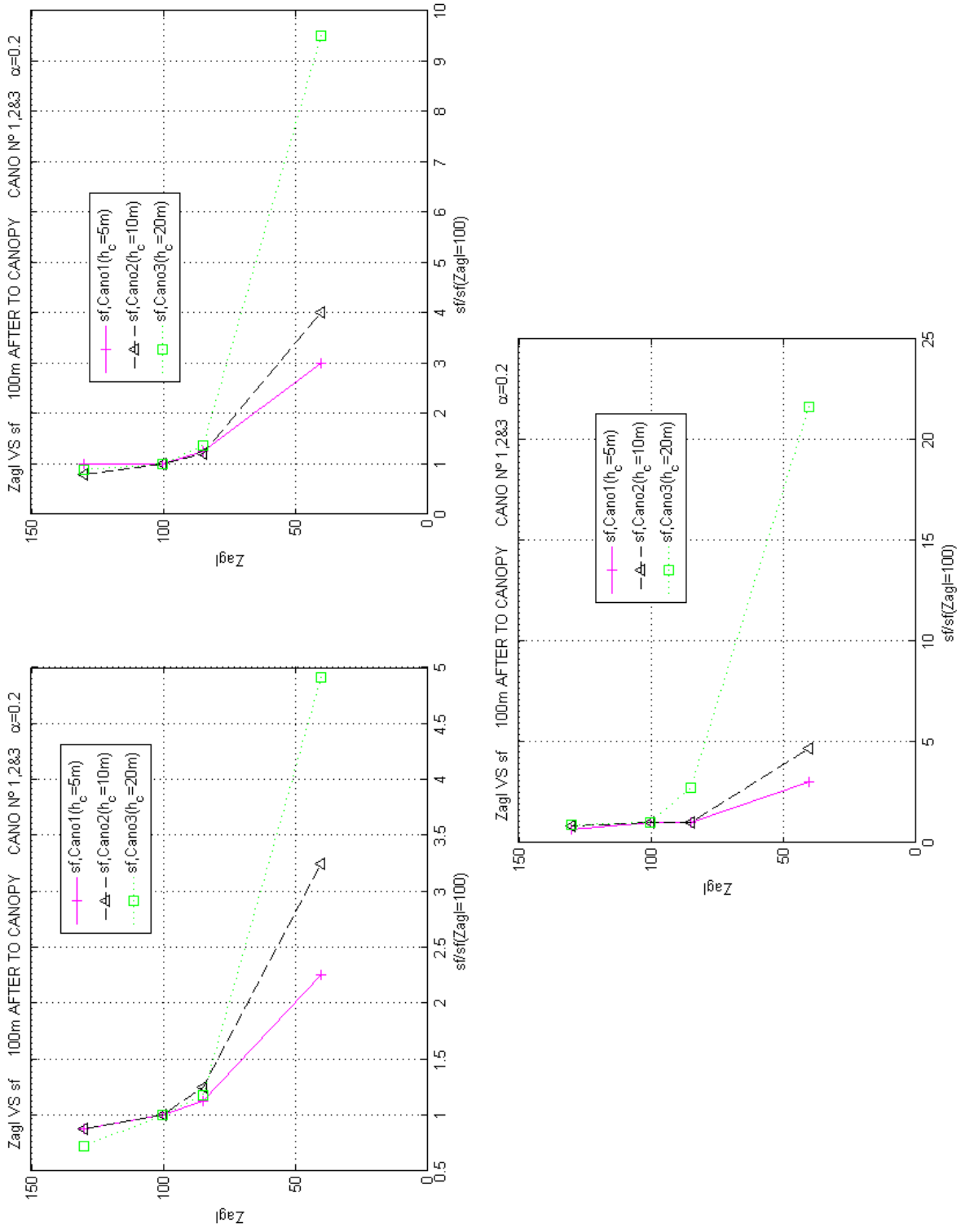

Figure 3.16: SF at x =100 m a.t.c., for Θ_b= +07°, +14° and +21°, c.f. top left

It is noticed that for h_c of 5 and 10 meters, the quantities of v_h, TI and SF vary somewhat (always referred to all the quantities obtained a $z_{agl} = 100\,\text{m}$), i.e., the terrain has no more influence than the forest canopy.

In contrast to $h_c = 20\,\text{m}$ are not predominant features of the forest canopy, the terrain effects are stronger and there is a considerable increasing for different bells.

Where this is most evident is from SF values, as shown in figure 3.17.

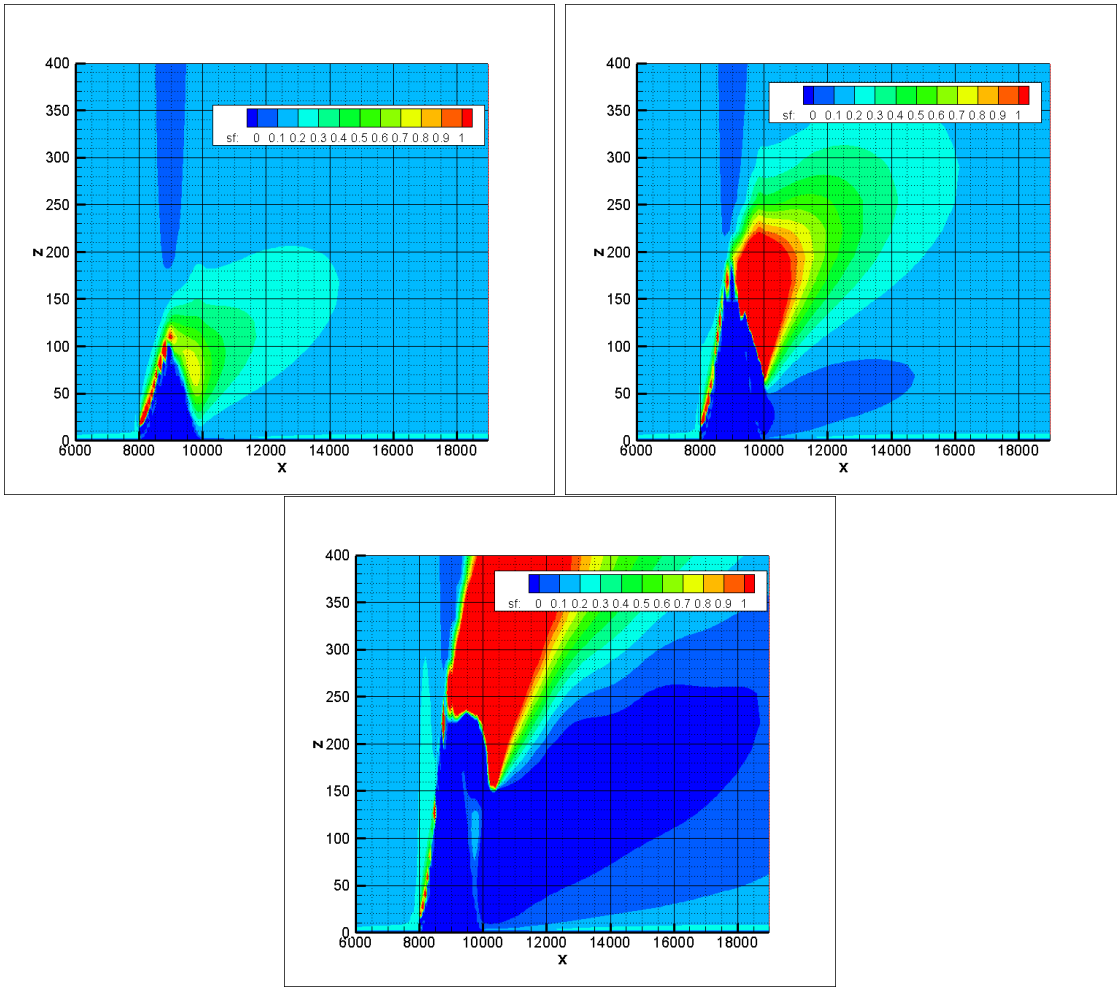

Figure 3.17: SF at $x = 100\,\text{m}$ a.t.c. for $h_c = 20\,\text{m}$, for $\Theta_b = +07°$, $+14°$and $+21°$, c.f. top left

.

Effect of leaf area idex, α

The differences in the values of v_h, TI and SF, for different α at 100 m a.t.c., are not negligible for $\Theta_b = 21°$: a linear evolution of quantities can be seen with the different α, as it is shown in figure 3.18.

For $\Theta_b = +7°$ and $\Theta_b = +14°$, there is a small influence of α in the behaviour of v_h, TI and SF, as it is shown in figures 3.19 and 3.20.

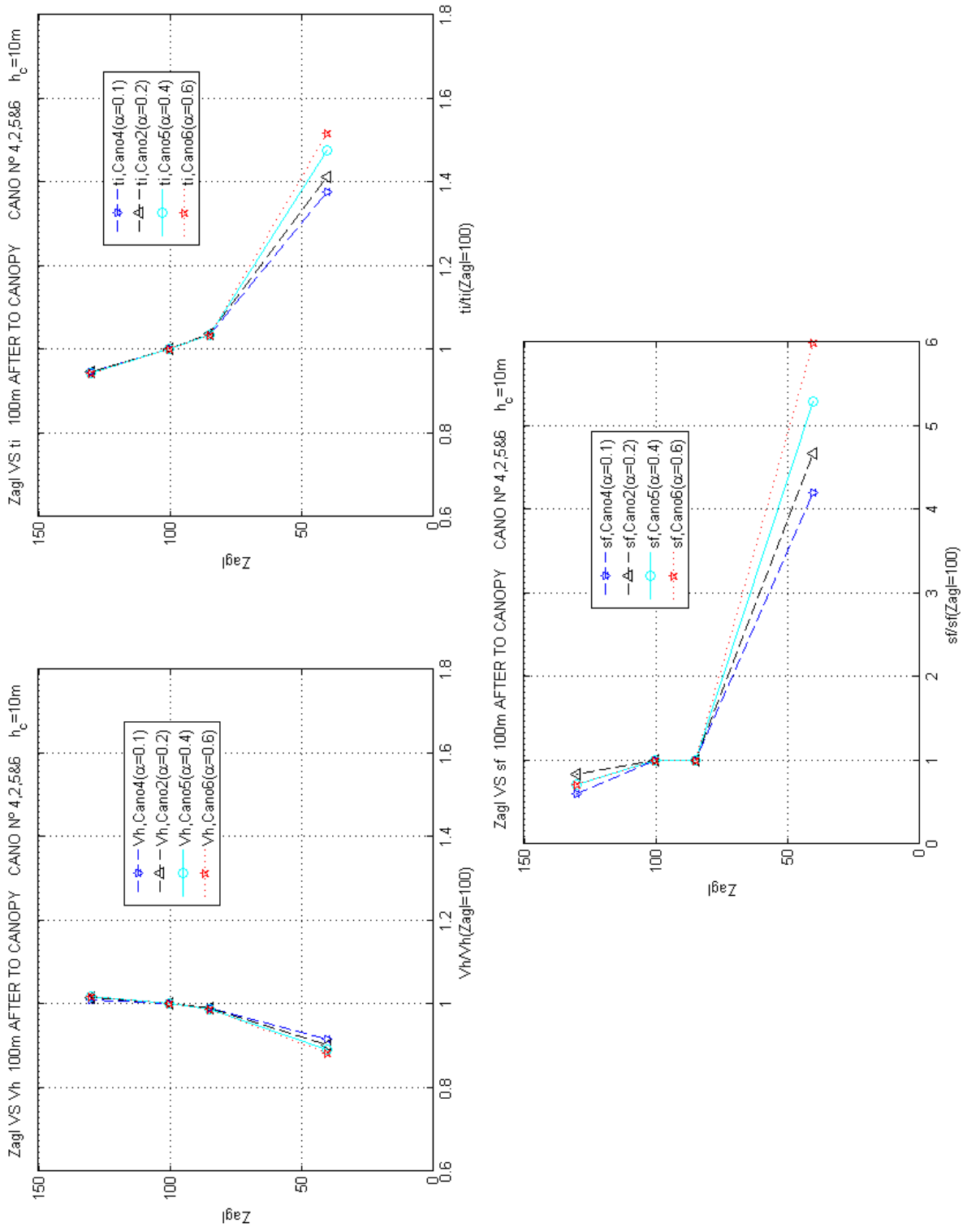

Figure 3.18: v_h, TI and SF at $x = 100\,\mathrm{m}$ a.t.c., for $\Theta_b = +21°$, depending on α.

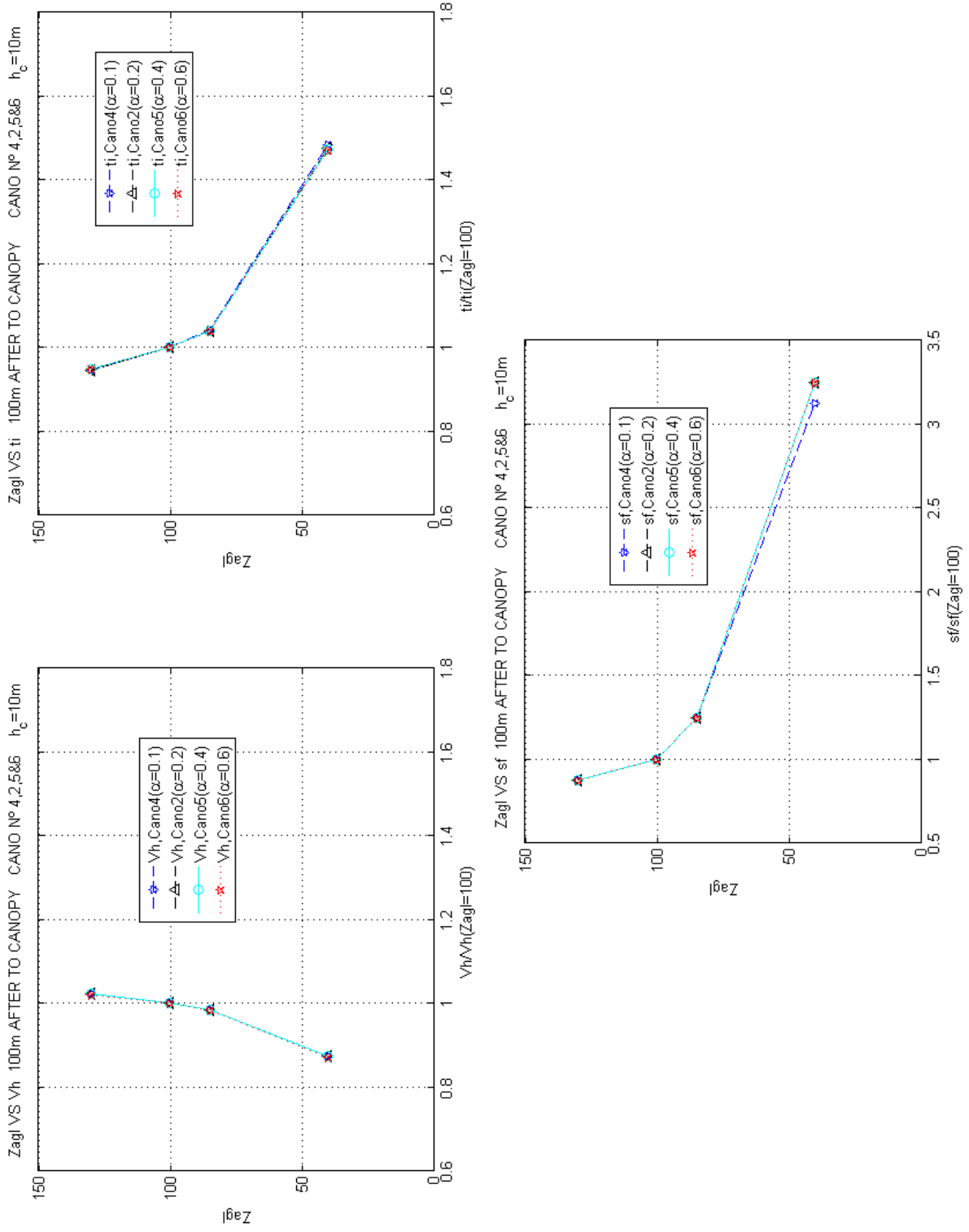

Figure 3.19: v_h, TI and SF at $x = 100\,\mathrm{m}$ a.t.c., for $\Theta_b = +07°$, depending on α.

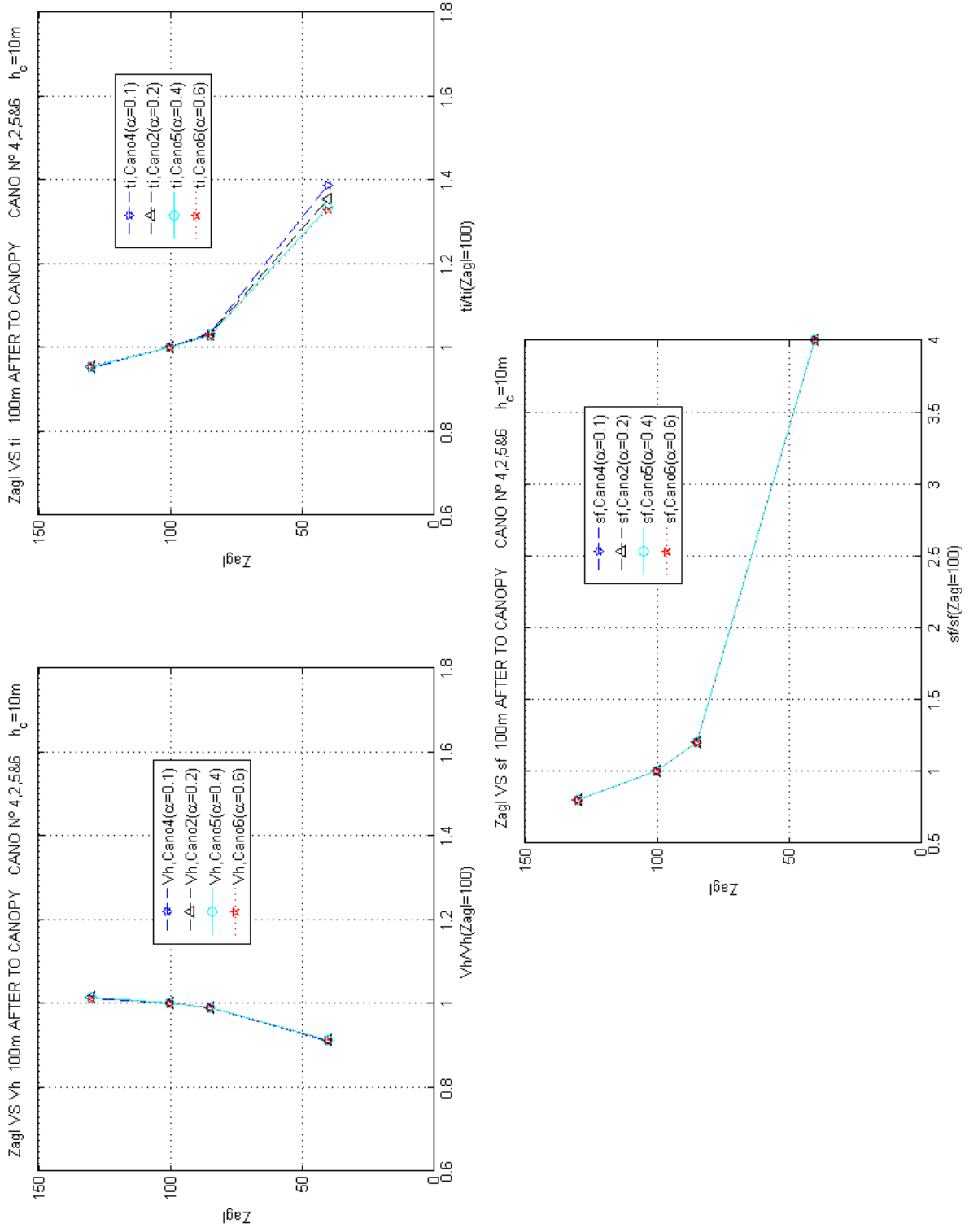

Figure 3.20: v_h, TI and SF at $x = 100\,\mathrm{m}$ a.t.c., for $\Theta_b = +14°$, depending on α.

Quantitative conclusions for positive bell terrain

As in the flat terrain, a guide from a practical point of view (of applicability) is attempted, obtaining quantitative results. The algebraic relations between wind flow parameters and forest canopy characteristics give rise to the construction of an abacus.

The little influence of the effect of the α is an important conclusion for the abacus construction. The $\alpha = 0.2$ was fixed in this analysis.

The following input variables: x, z_{agl}, v_h, TI and SF, and the output variable is the h_c have been considered.

In line with the previous paragraph, the following figures, 3.21, 3.24, 3.22, 3.25, 3.23 and 3.26, show that the evolution of v_h decreases, the increase of TI and the increase of SF, for different h_c and for various distances a.t.c..

Finally, the abacus are created summarizing this information and establishing relationships at constant z_{agl} and between wind flow parameters and h_c.

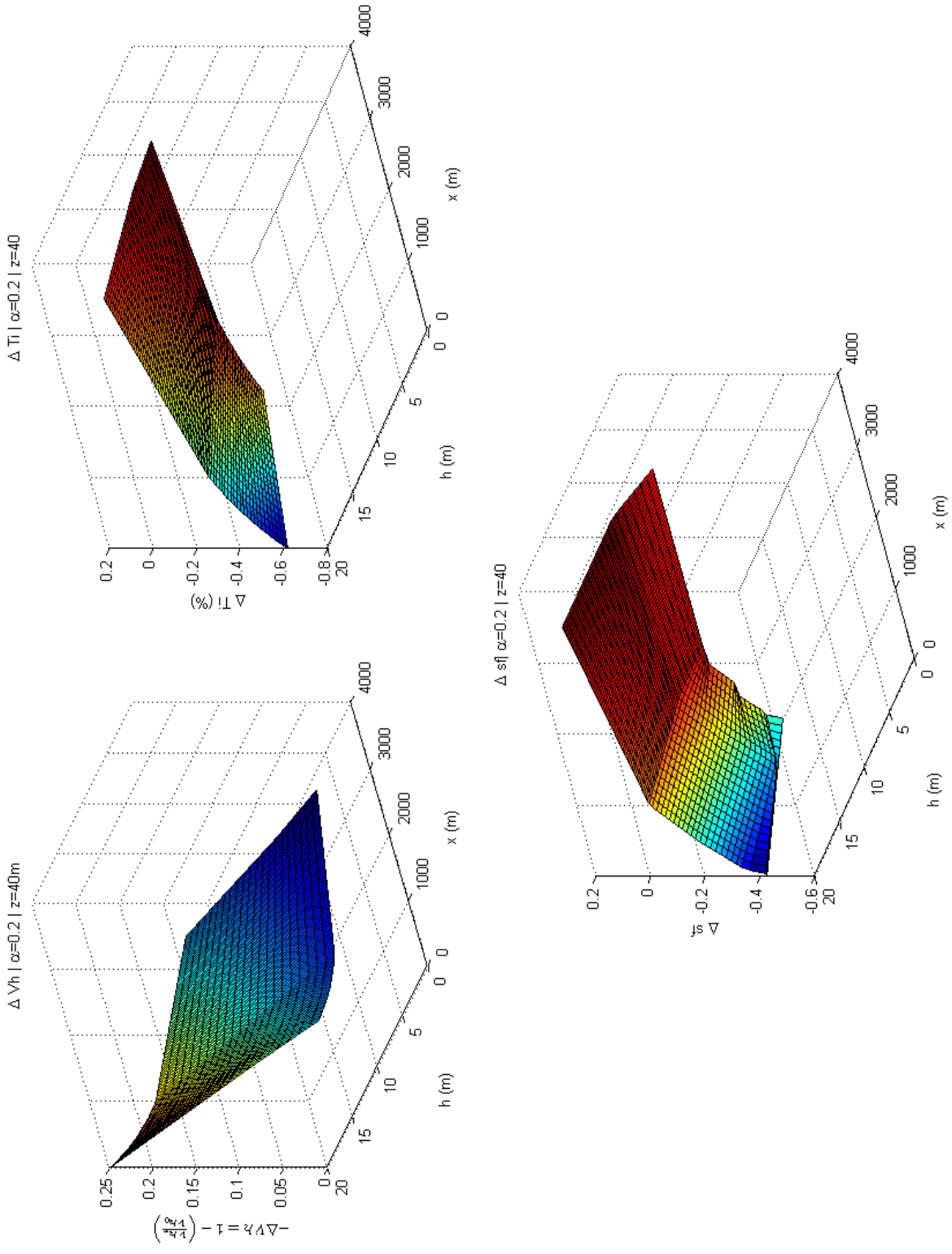

Figure 3.21: v_h, TI and SF, depending on h_c, $BT_{+07°}$, at z_{agl}= 40 m

.

Figure 3.22: v_h, TI and SF, depending on h_c, $BT_{+14°}$, at z_{agl}= 40 m

.

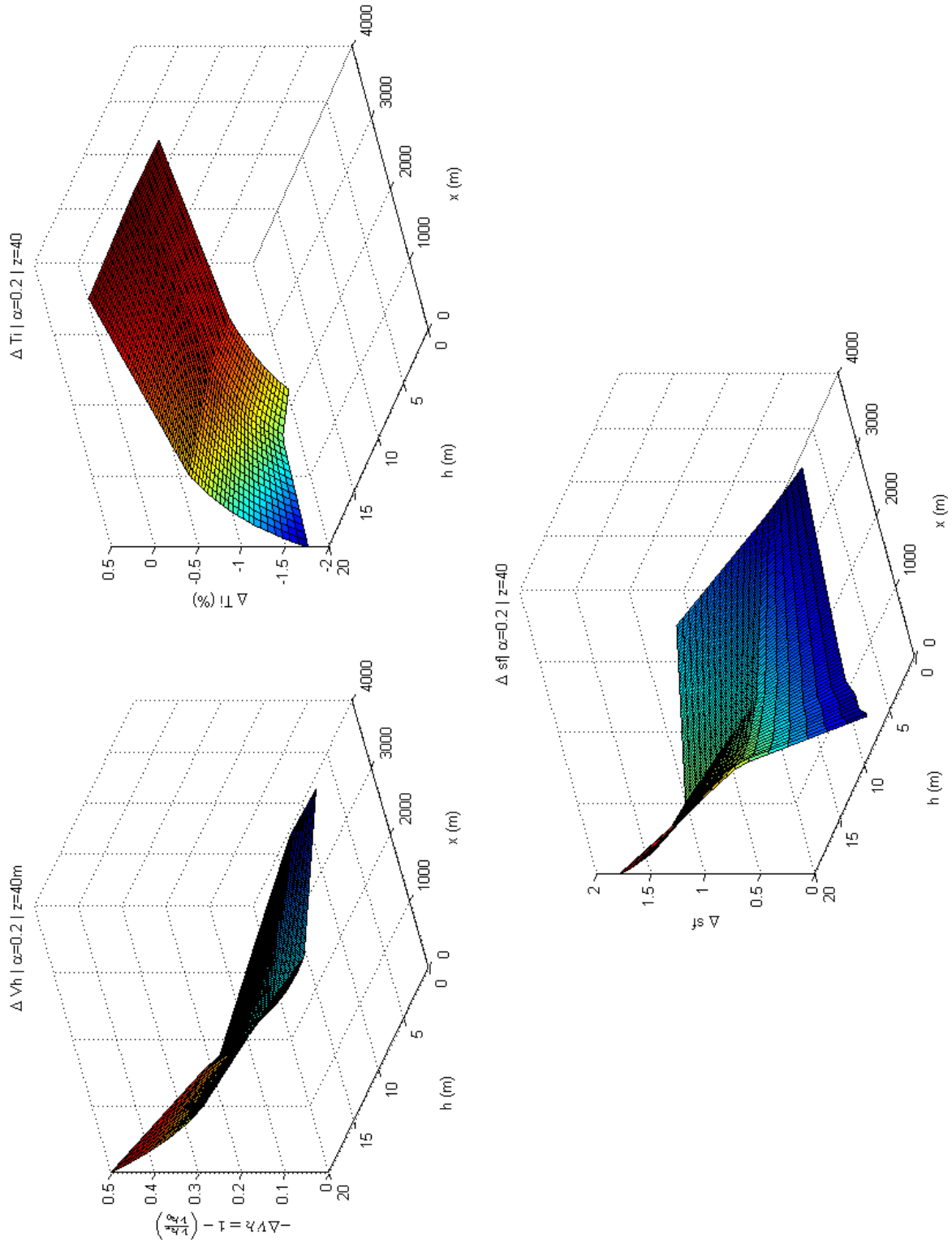

Figure 3.23: v_h, TI and SF, depending on h_c, $BT_{+21°}$, at z_{agl}= 40 m

.

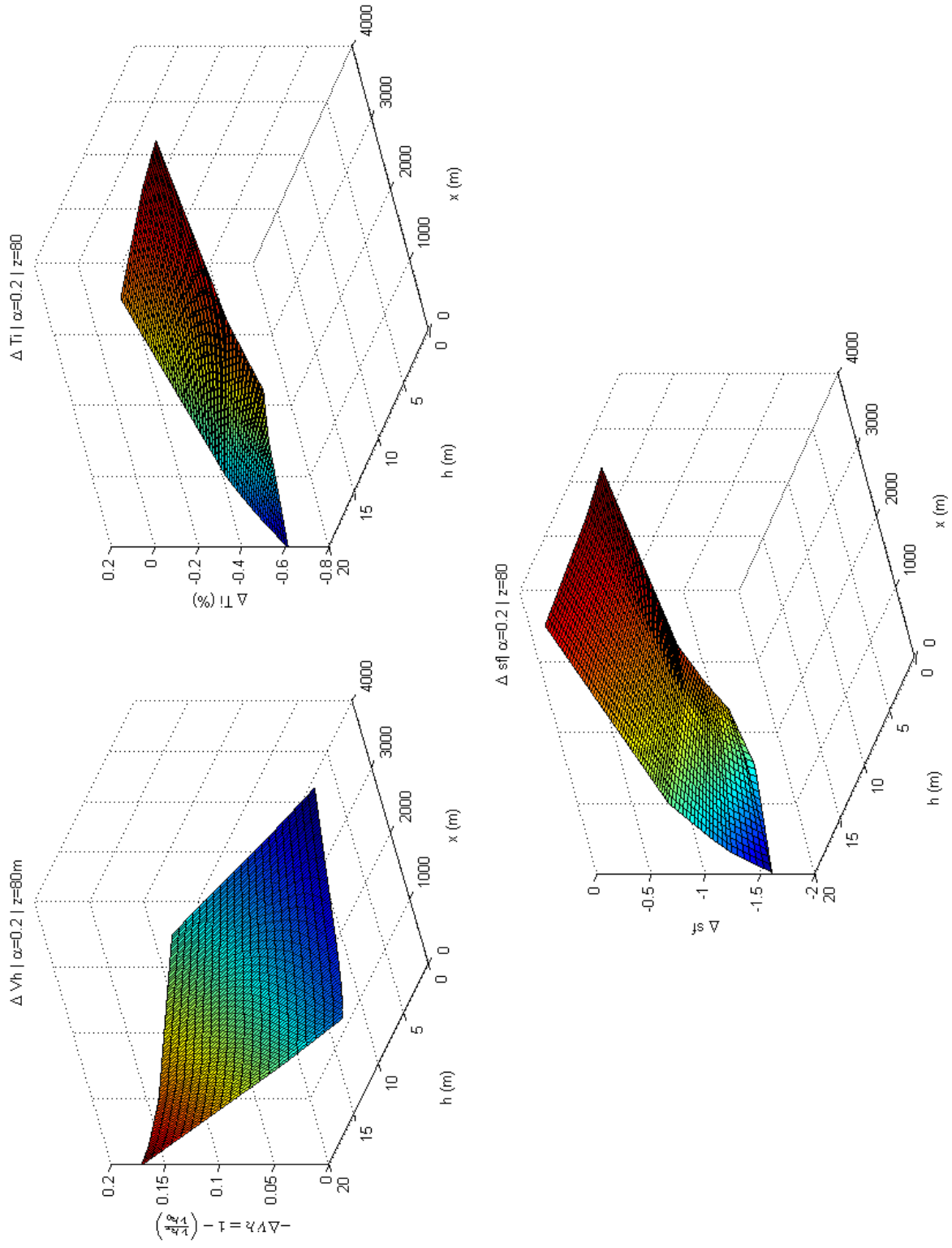

Figure 3.24: v_h, TI and SF, depending on h_c, $BT_{+07°}$, at z_{agl}= 80 m

.

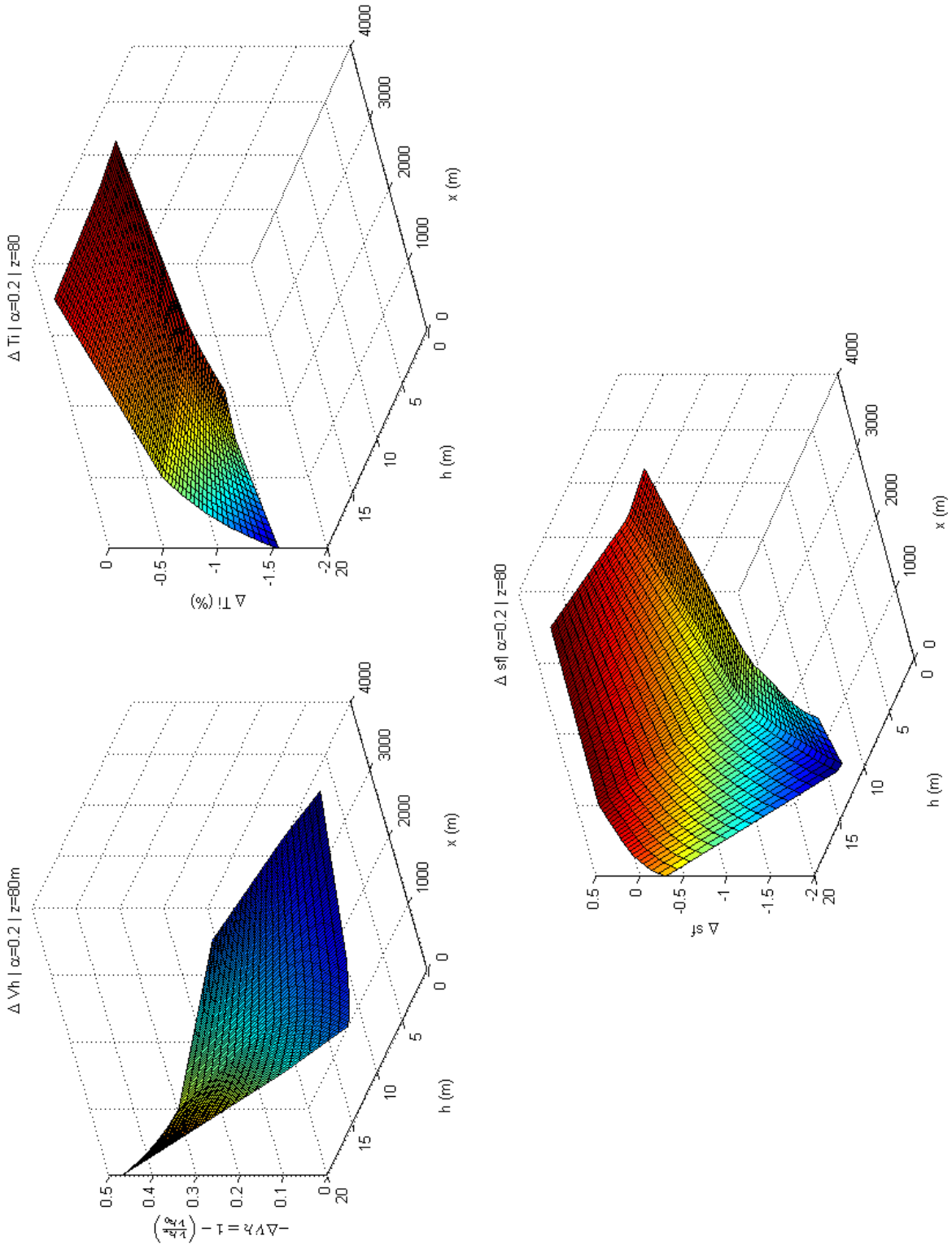

Figure 3.25: v_h, TI and SF, depending on h_c, $BT_{+14°}$, at z_{agl}= 80 m

.

Figure 3.26: v_h, TI and SF, depending on h_c, $BT_{+21°}$, at z_{agl}= 80 m

.

3.3.2 Negative bell terrain.

In the following subsection, the h_c and α effects of the wind flow are investigated for the bell terrain with forest on the negative slope this time.

Effects of forest canopy height, h_c.

For $x = 100\,\text{m}$ a.t.c., the magnitudes of v_h and TI (referred to those obtained 100 m a.g.l.) are practically invariable for the three Θ_b, as it is shown in figures 3.27, 3.28 and 3.29. And for SF with $h_c = 20\,\text{m}$ there is more influence of the terrain, and $h_c = 5\,\text{m}$ and $h_c = 10\,\text{m}$, the SF does not practically change.

For $x = 1000\,\text{m}$ a.t.c., magnitudes of v_h and TI (which are non-dimensionalised by their values at 100 m a.g.l.) for Θ_b=-7° and Θ_b=-14° change slightly for each h_c studied, ie, there is a predominance of the forest canopy versus terrain.

However, with Θ_b=-21° an inversion of the predominance was produced for h_c= 10 m and h_c= 20 m, i.e., the effects on wind flow of forest decrease and the importance of terrain increases.

In the same way, as for the positive Θ_b, the influence of terrain starts to be visible at higher h_c, i.e., for a higher h_c a minimal change in slope is more susceptible to change the tendency of the magnitudes of v_h and TI.

The SF behaviour has been influenced by the terrain for all h_c. See figures 3.30, 3.31 and 3.32.

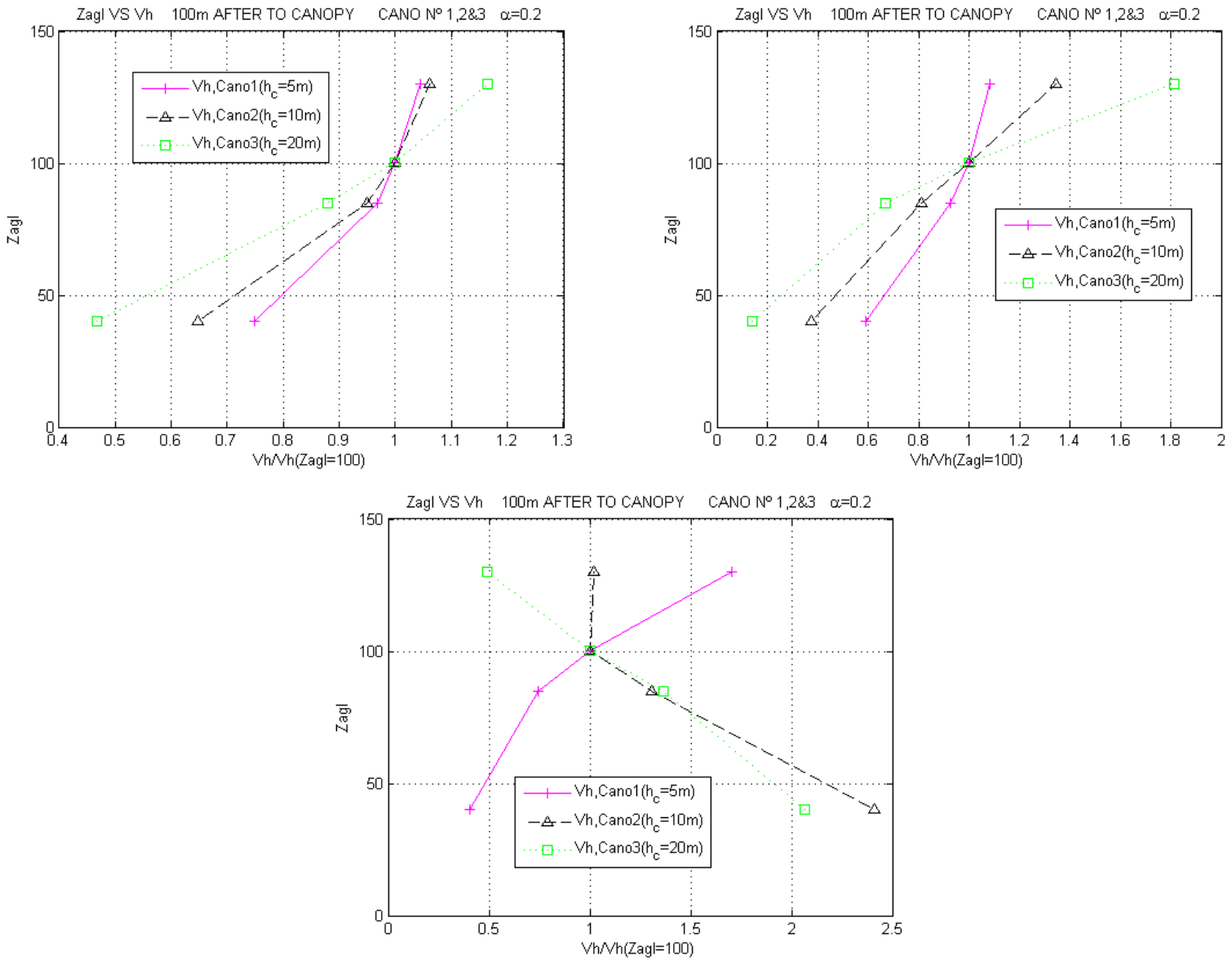

Figure 3.27: v_h at x =100 m a.t.c., depending on h_c, c.f. top left: Θ_b=-07°, -14°and -21°

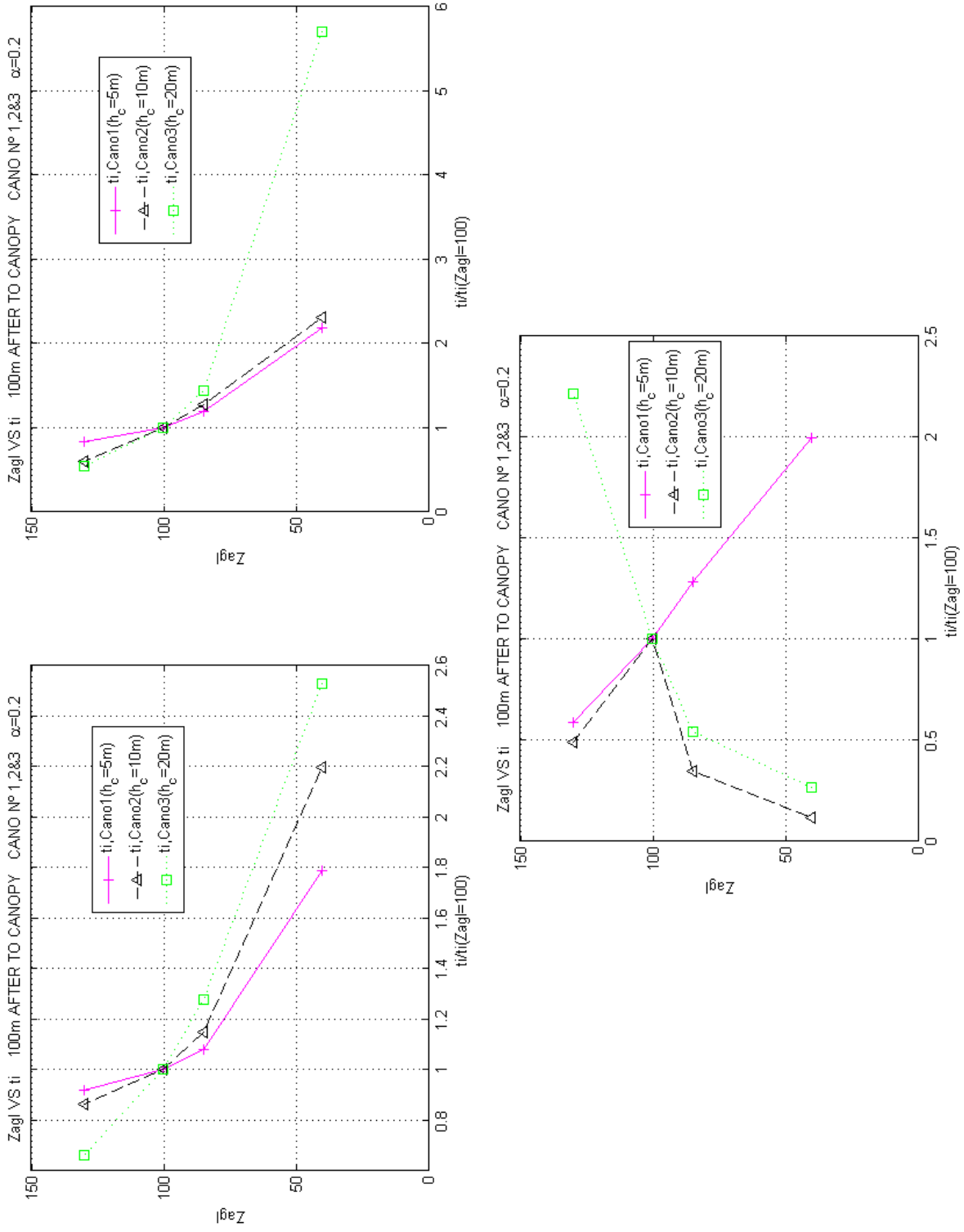

Figure 3.28: TI at x =100 m a.t.c., depending on h_c, c.f. top left: Θ_b= -07°, -14°and -21°

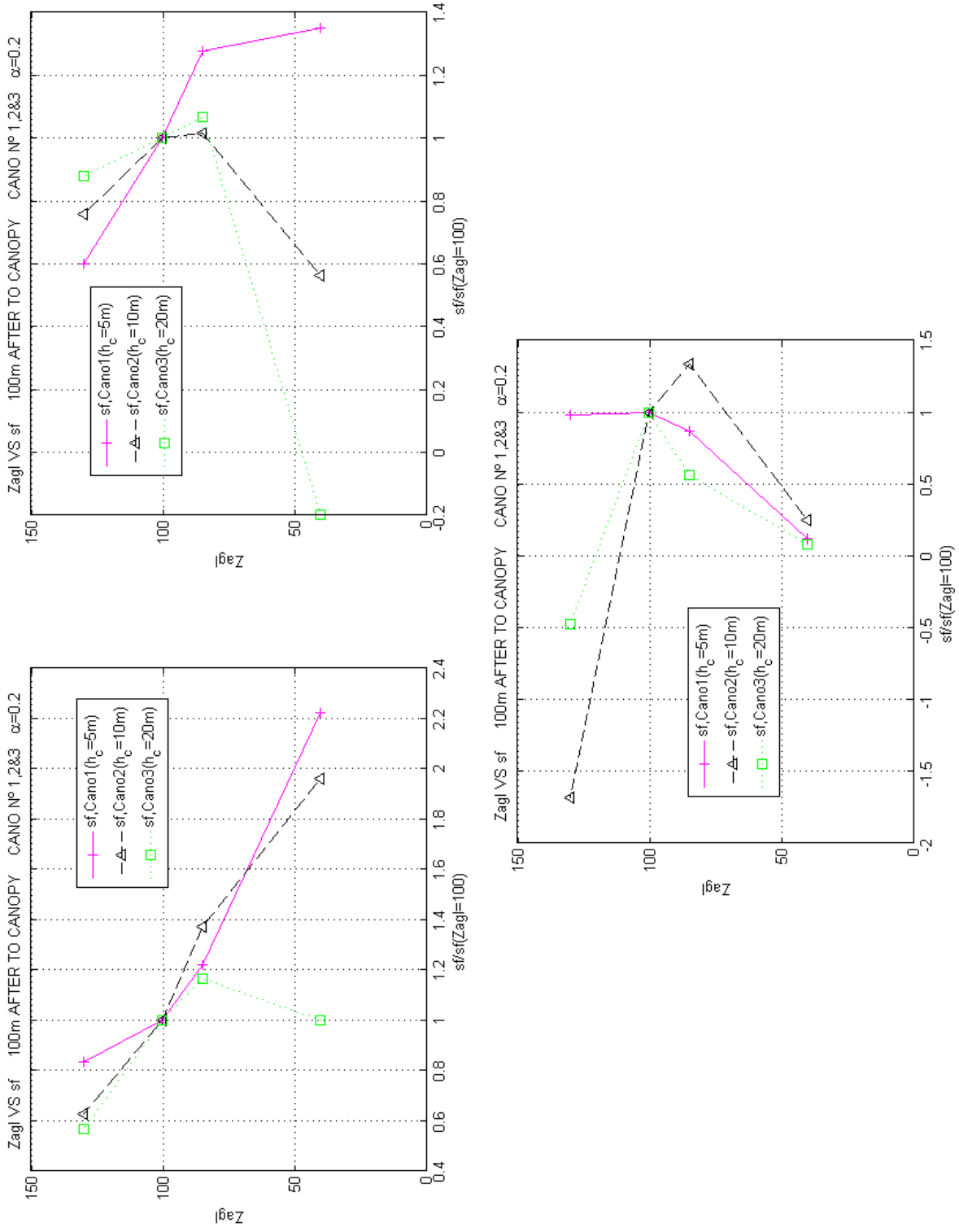

Figure 3.29: SF at x =100 m a.t.c., depending on h_c, c.f. top left: Θ_b= -07°, -14°and -21°

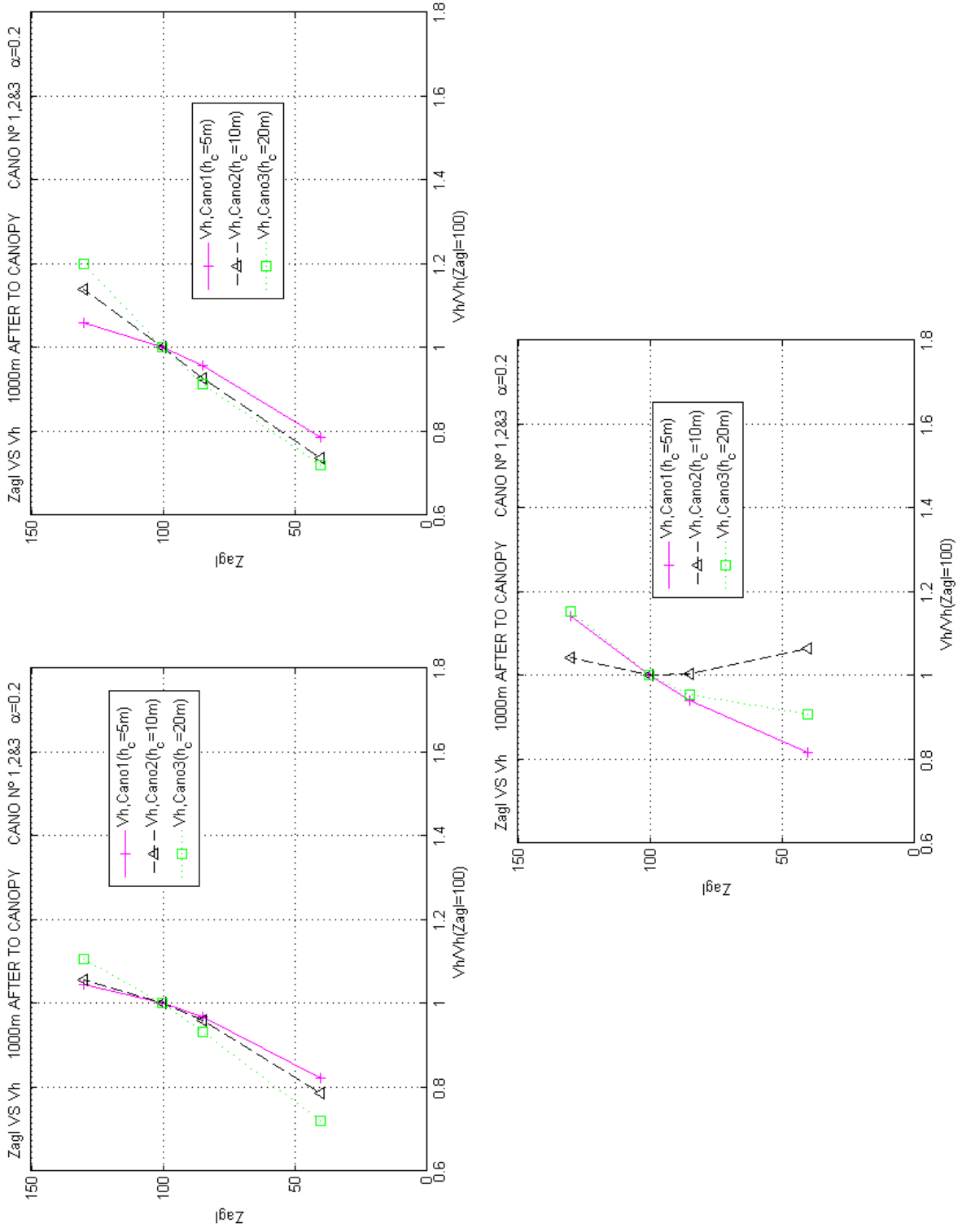

Figure 3.30: v_h at x =1000 m a.t.c., depending on h_c, c.f. top left: Θ_b= -07°, -14°and -21°

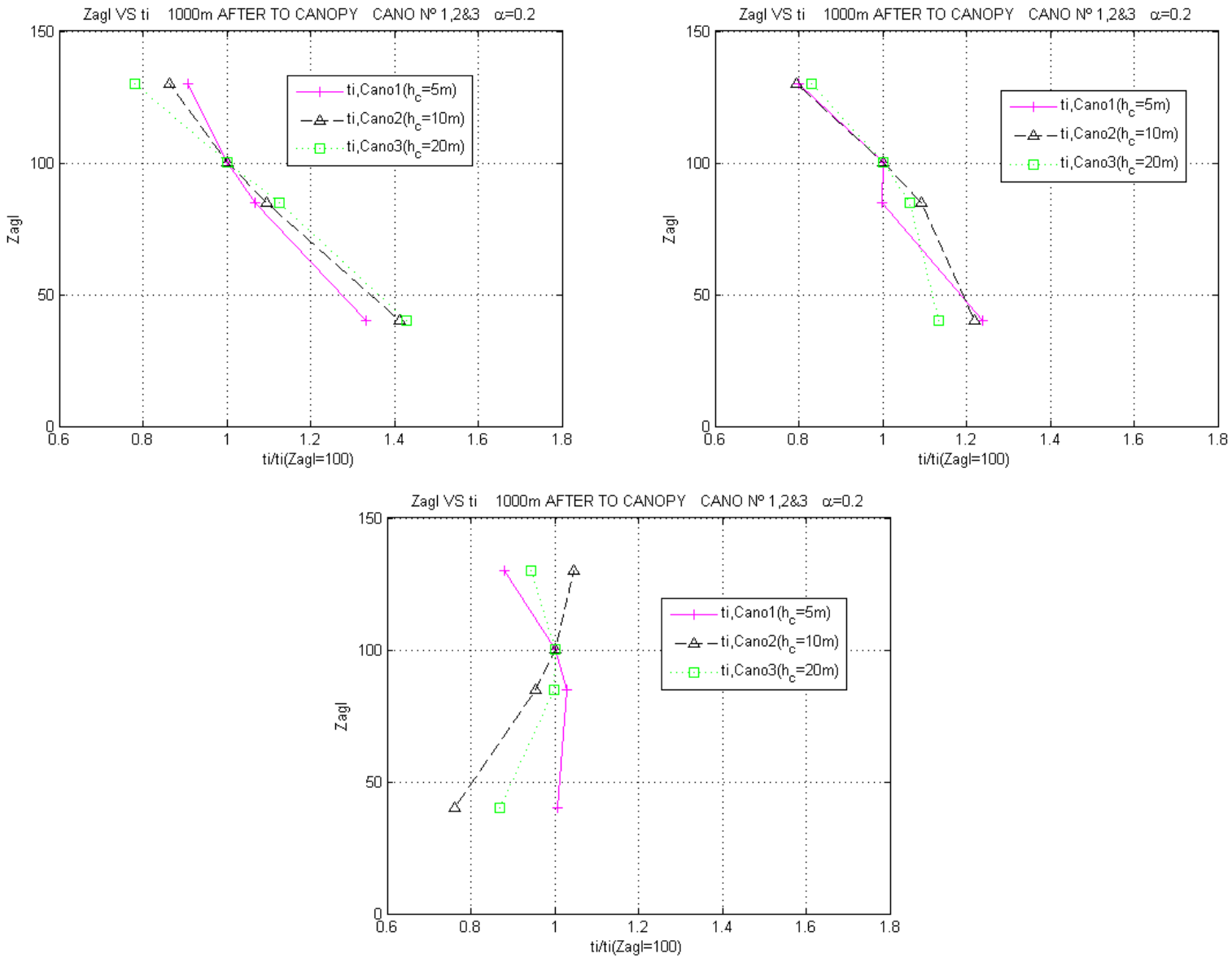

Figure 3.31: TI at x =1000 m a.t.c., depending on h_c, c.f. top left: Θ_b=-07°, -14°and -21°

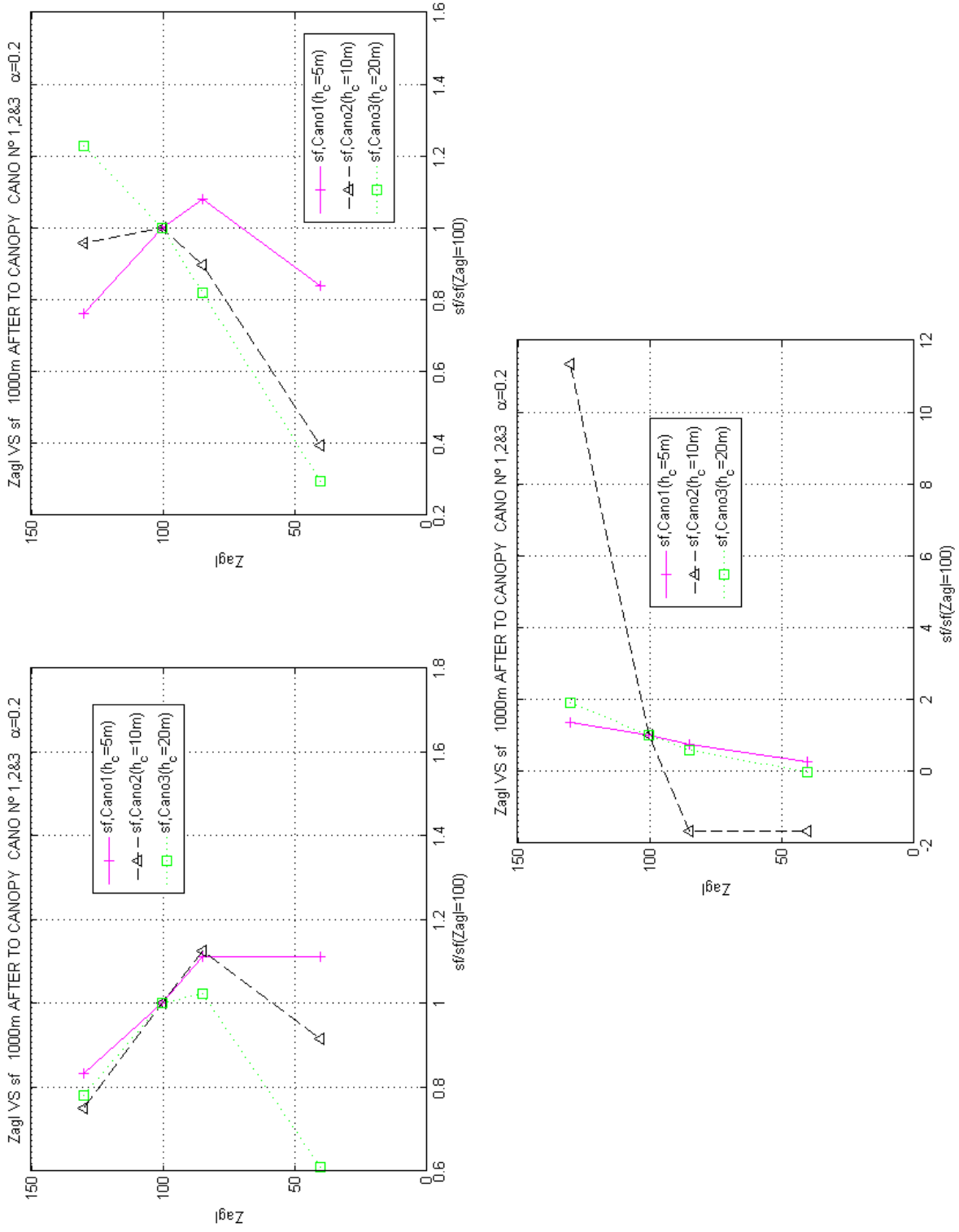

Figure 3.32: SF at x =1000 m a.t.c., depending on h_c, c.f. top left: Θ_b= -07°, -14° and -21°

Effects of leaf area index, α.

For $x = 100$ m a.t.c., the values of v_h and TI (referred to those obtained 100 m a.g.l.) are invariable for the three Θ_b.

The SF has a similar behaviour that v_h and TI at a distance from $x = 1000$ m a.t.c., referring to the predominance of the forest canopy for terrain with slopes of Θ_b=-7°, Θ_b=-14°and Θ_b=-21°.

For $x = 1000$ m a.t.c., magnitudes of v_h and TI (referred to those obtained 100 m a.g.l.) for Θ_b=-7°and Θ_b=-14°change a bit for all α's that have been studied, ie, there is predominance of the canopy. But for Θ_b=-21°, the influence of the terrain comes into prominance, as shown in Figures 3.33 and 3.34.

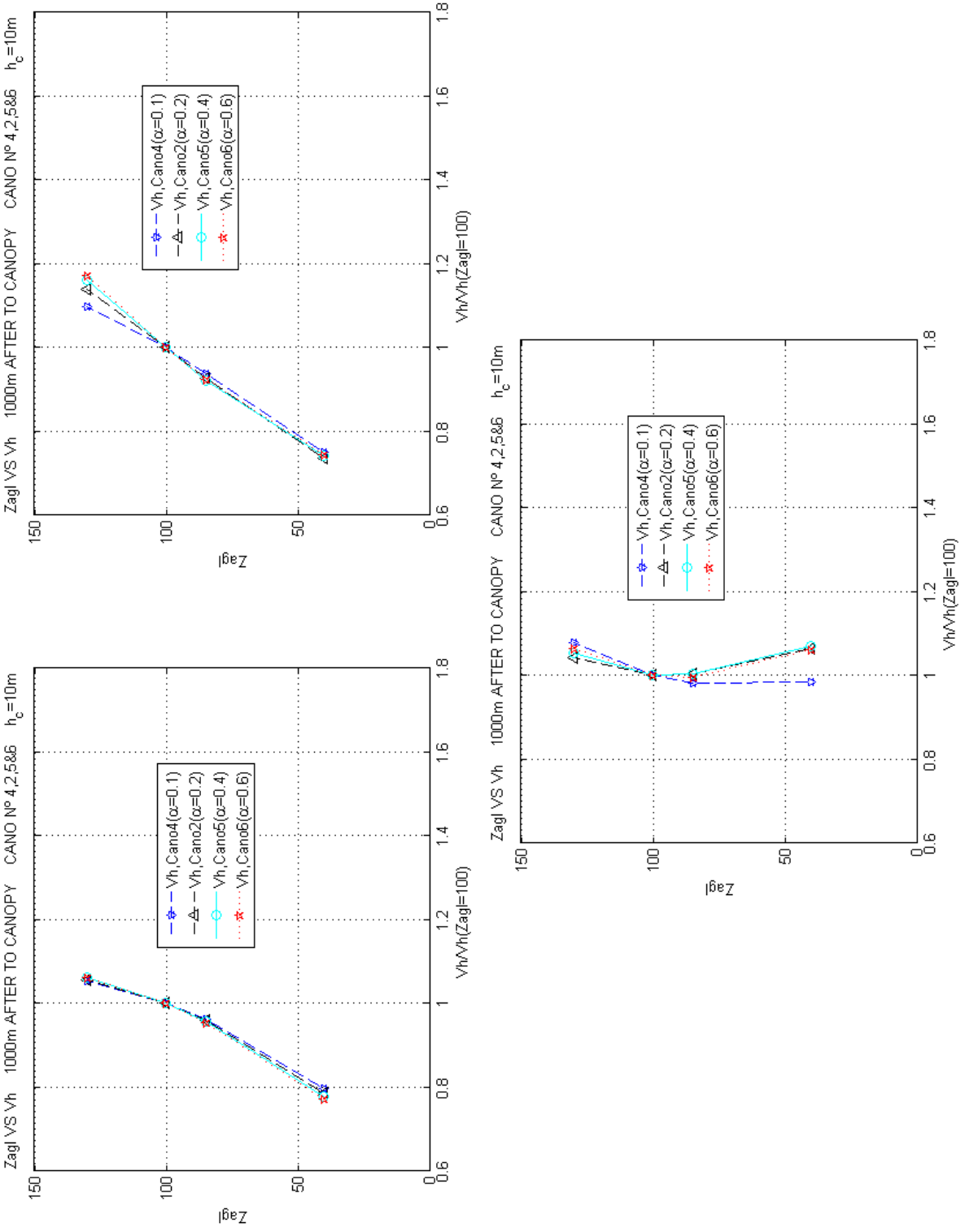

Figure 3.33: v_h $x = 1000\,\mathrm{m}$ a.t.c., varying Θ_b, depending on α.

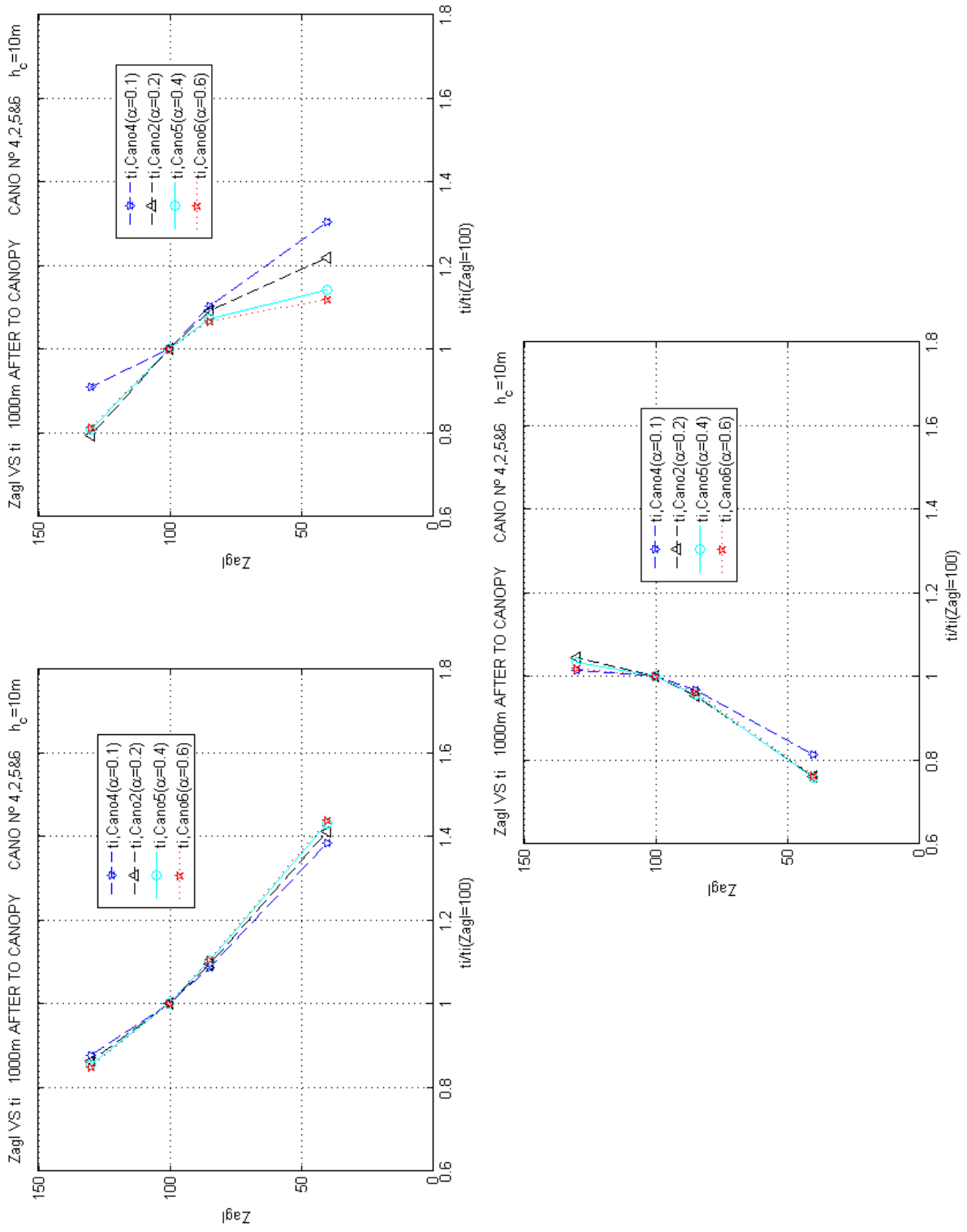

Figure 3.34: TI $x = 1000\,\mathrm{m}$ a.t.c., varying Θ_b, depending on α.

Quantitative conclusions for negative bell terrrain

As in the flat terrain and positive bell terrain, a guide from a practical point of view (of applicability) is tackled, obtaining conclusions of mathematical order. The algebraic relations (polynomials) between wind flow parameters and forest canopy characteristics give rise to the possible construction of an abacus.

The little influence of the effect of α is an important conclusion for the abacus construction, it was therefore removed as a variable, and a value of $\alpha = 0.2$ was fixed in this analysis.

The following input variables: x, z_{agl}, v_h, TI and SF, and the output variable is the h_c have been considered.

In line with the previous paragraph, the following figures, 3.35, 3.36, 3.37, 3.38, 3.39 and 3.40, show the decrease of v_h, the increase of TI and the increase of SF, for growing h_c and for various distances a.t.c..

Finally, the abacuses are created summarizing this information and establishing relationships at z_{agl}, between wind flow parameters measured on site and h_c.

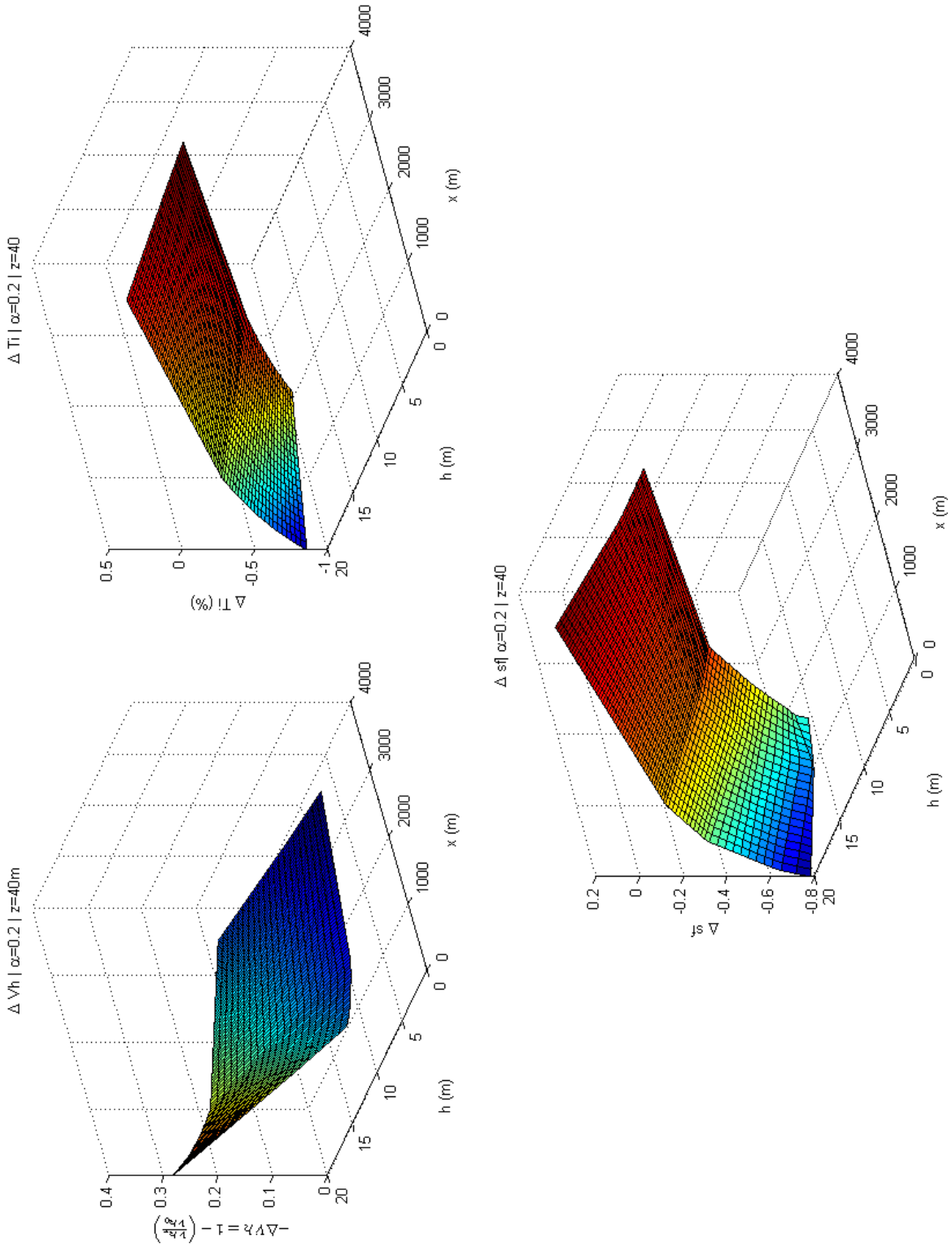

Figure 3.35: v_h, TI and SF, depending on h_c, $BT_{-07°}$. For z_{agl}= 40 m

.

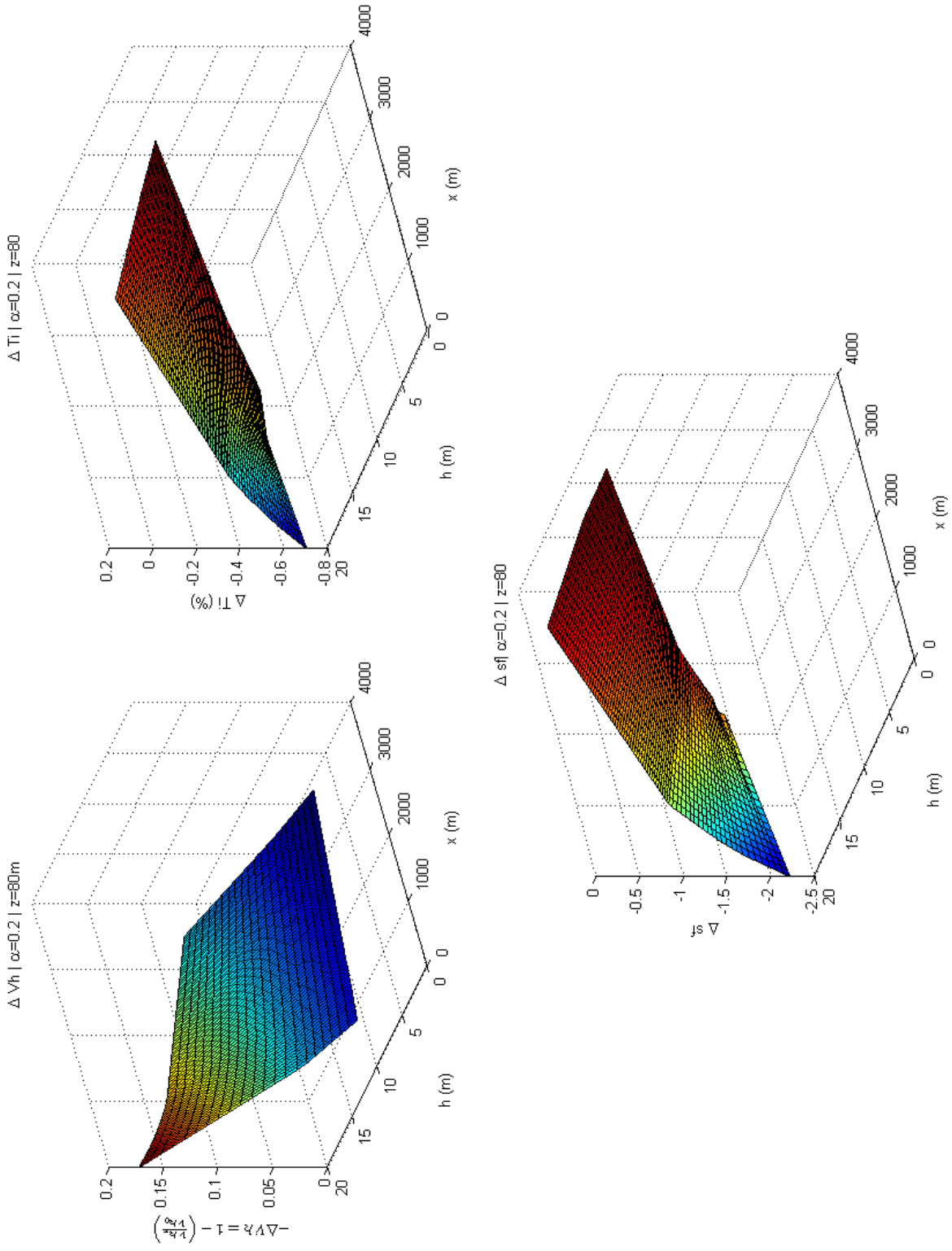

Figure 3.36: v_h, TI and SF, depending on h_c, $\mathrm{BT}_{-07°}$. For z_{agl}= 80 m

.

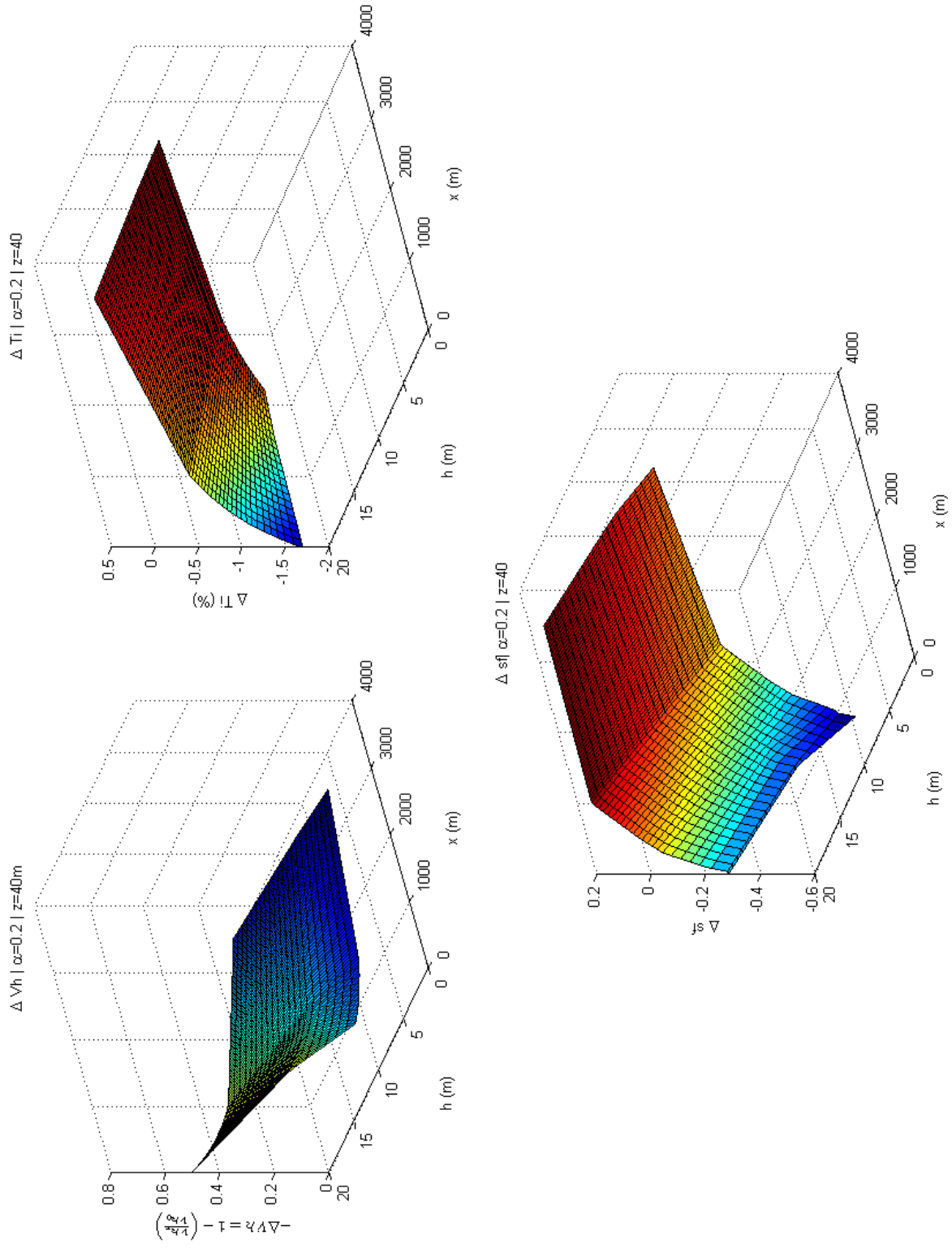

Figure 3.37: v_h, TI and SF, depending on h_c, $BT_{-14°}$. For z_{agl}= 40 m

.

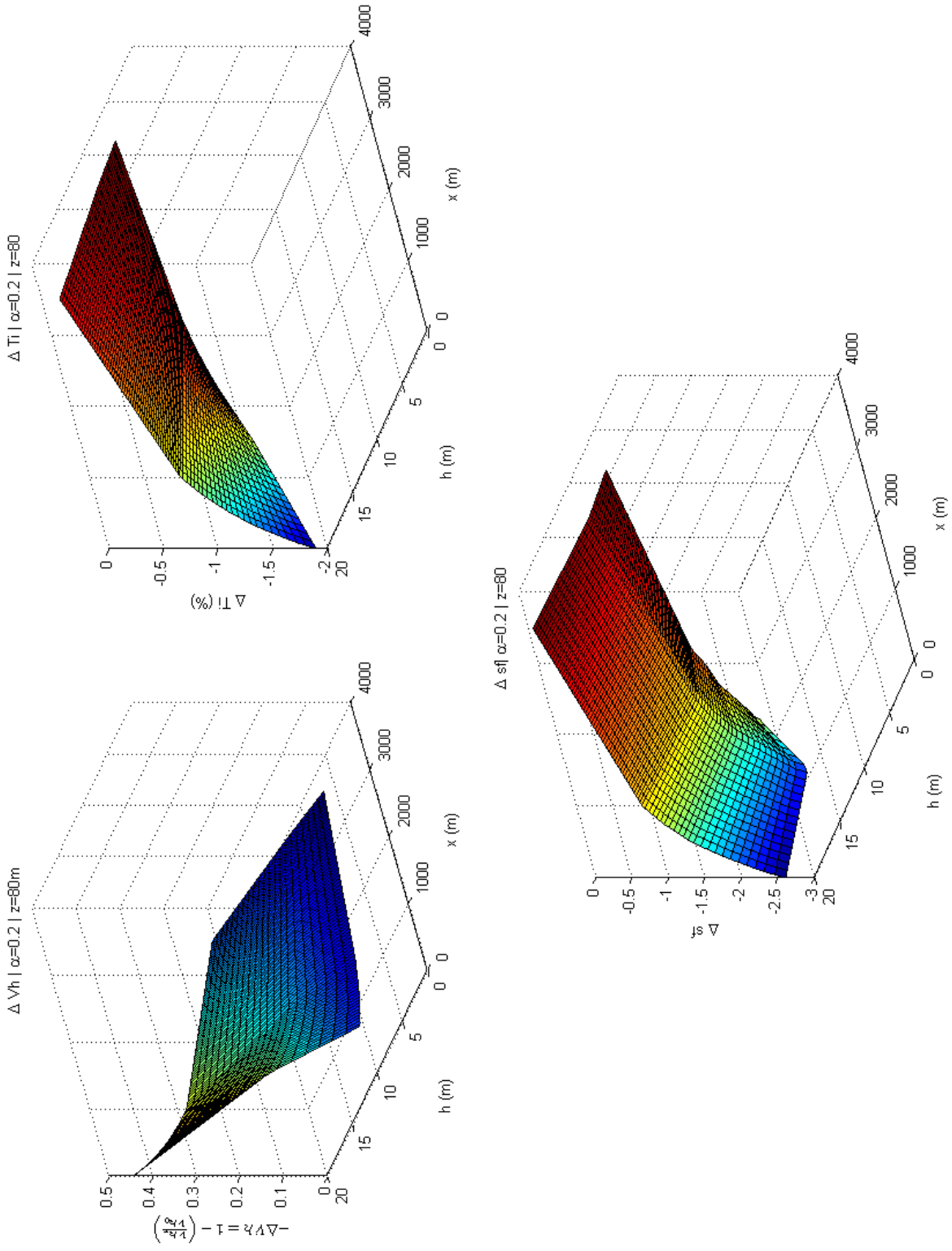

Figure 3.38: v_h, TI and SF, depending on h_c, $\mathrm{BT}_{-14°}$. For z_{agl}= 80 m

.

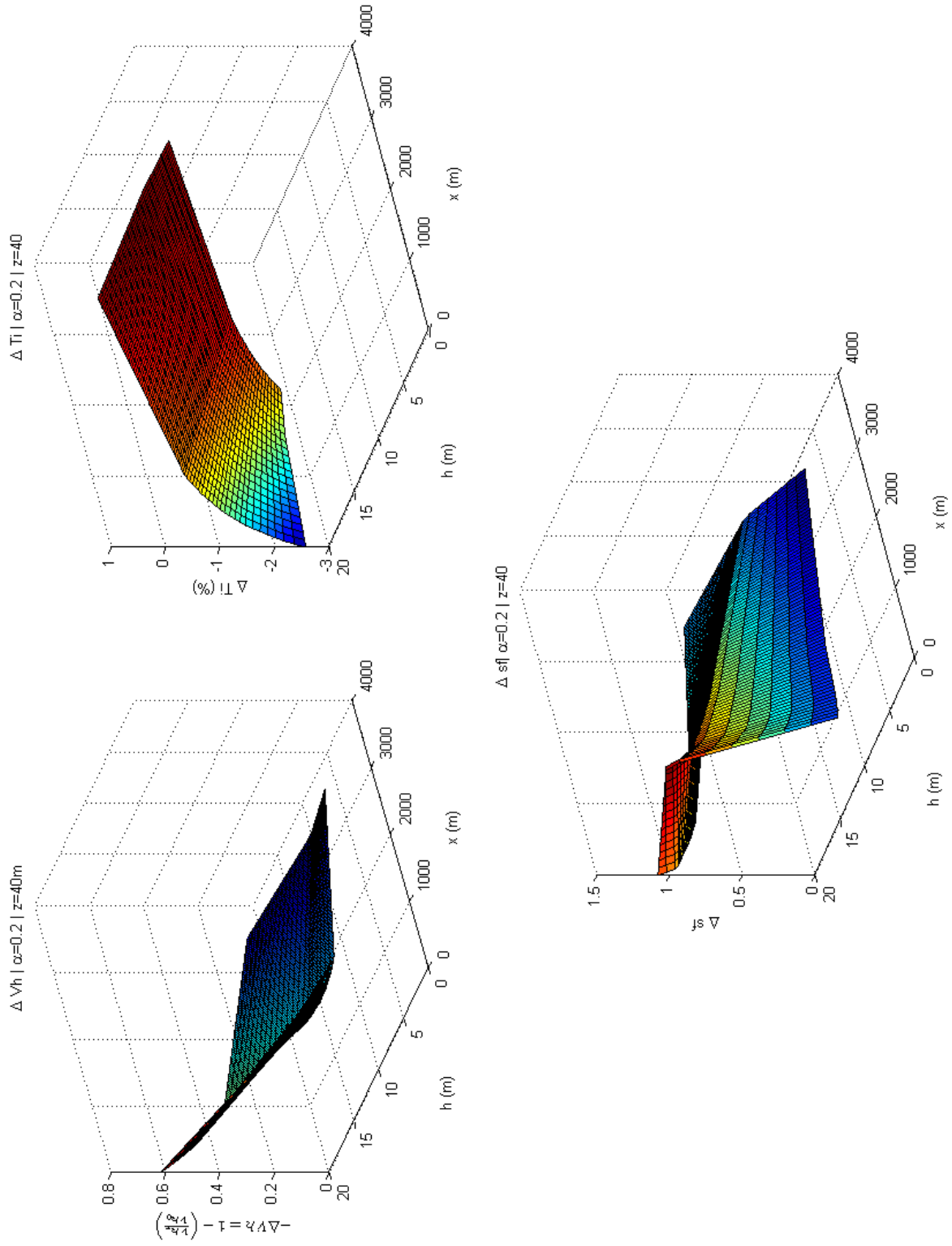

Figure 3.39: v_h, TI and SF, depending on h_c, $BT_{-21°}$. For z_{agl}= 40 m

.

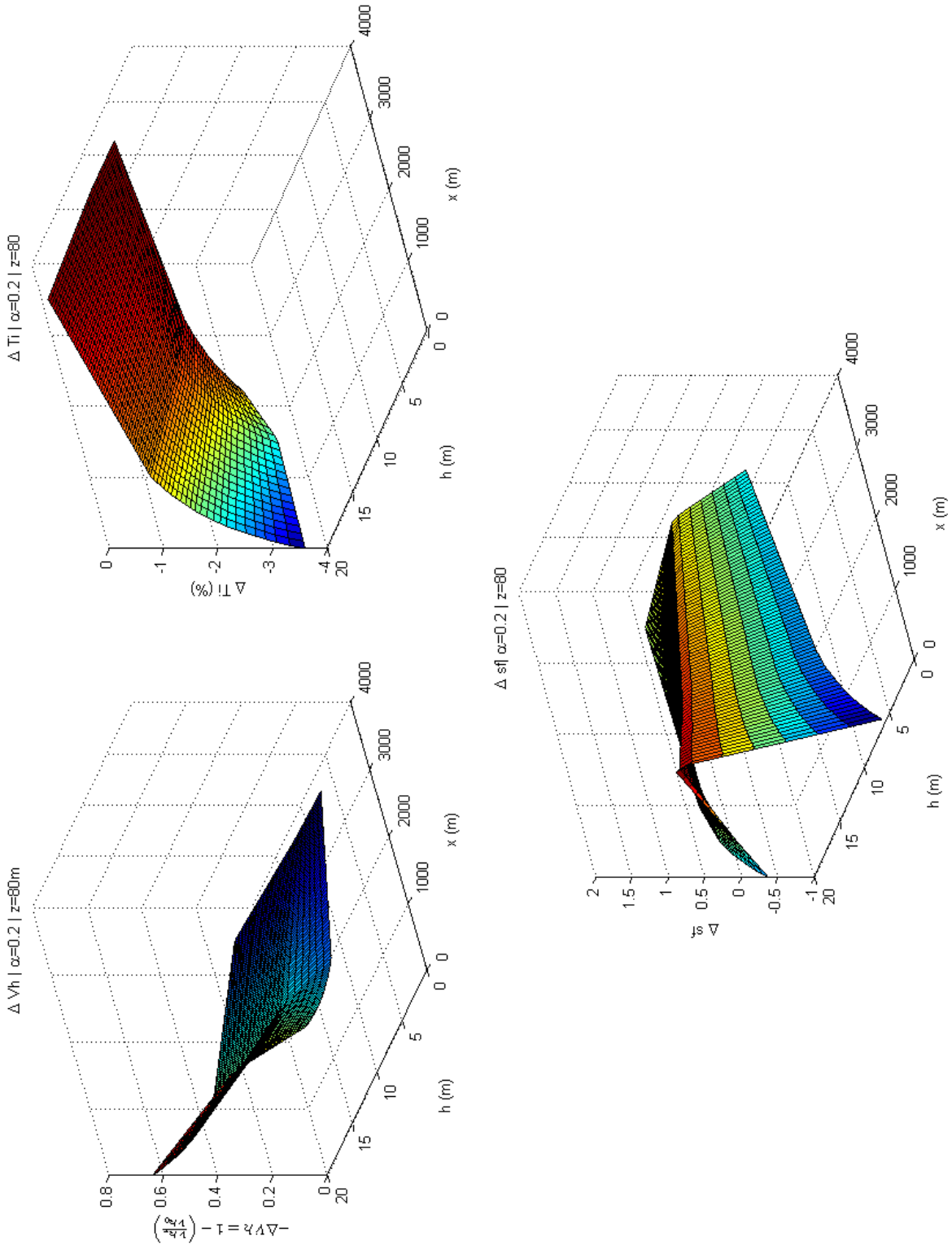

Figure 3.40: v_h, TI and SF, depending on h_c, $\mathrm{BT}_{-21°}$. For z_{agl}= 80 m

.

3.4 Conclusions of the parametric study

The main objective for this chapter was to know the theoretical wind flow behaviour, in particular v_h, TI and SF. The chapter is the base for the practical study and to optimize the use of forest canopy models.

The main conclusion for this chapter is that the influence of α is negligible for wind flow behaviour.

Chapter 4

Case study: ALEXANDROVO

4.1 Introduction and motivation

This chapter aims to establish a validation of the empirical models defined in the previous chapter, with a real case. Therefore, the abacus developed in Chapter 3 were applied to the wind farm project studied by MEGAJOULE (MJ) in the Northeast of Bulgaria, called Alexandrovo-Wind Farm (A-WF).

This project was selected because it contains several forest patches and its topography is relatively simple with moderate terrain slopes. The forest consists of three levels (8, 10 and 12 m) defined previously. These will be checked a posteriori.

The main aim of this study is to improve the method for estimating the height of canopy forests when the forest characteristics are unknown.

4.2 General description

4.2.1 Site location

The A-WF project is located in the municipallity of Turgovishte, in the north-eastern of Bulgaria, whithin about 95 km east and 130 km west from the Romania border and from the Bulgarian coastline with the Black Sea, respectively.

The prospect wind farm area extends for almost 20 km over gently hilly agricultural land. The site has altitudes ranging from 440 to 520 m a.s.l. approximately.

Figure 4.1: General location of Alexandrovo

4.2.2 Terrain description

The area consists of agricultural land mostly covered with low to medium vegetation but surrounded by various forest patches. There are also some distant villages in the proximity.

Figure 4.2: Examples of surrounding area and cover

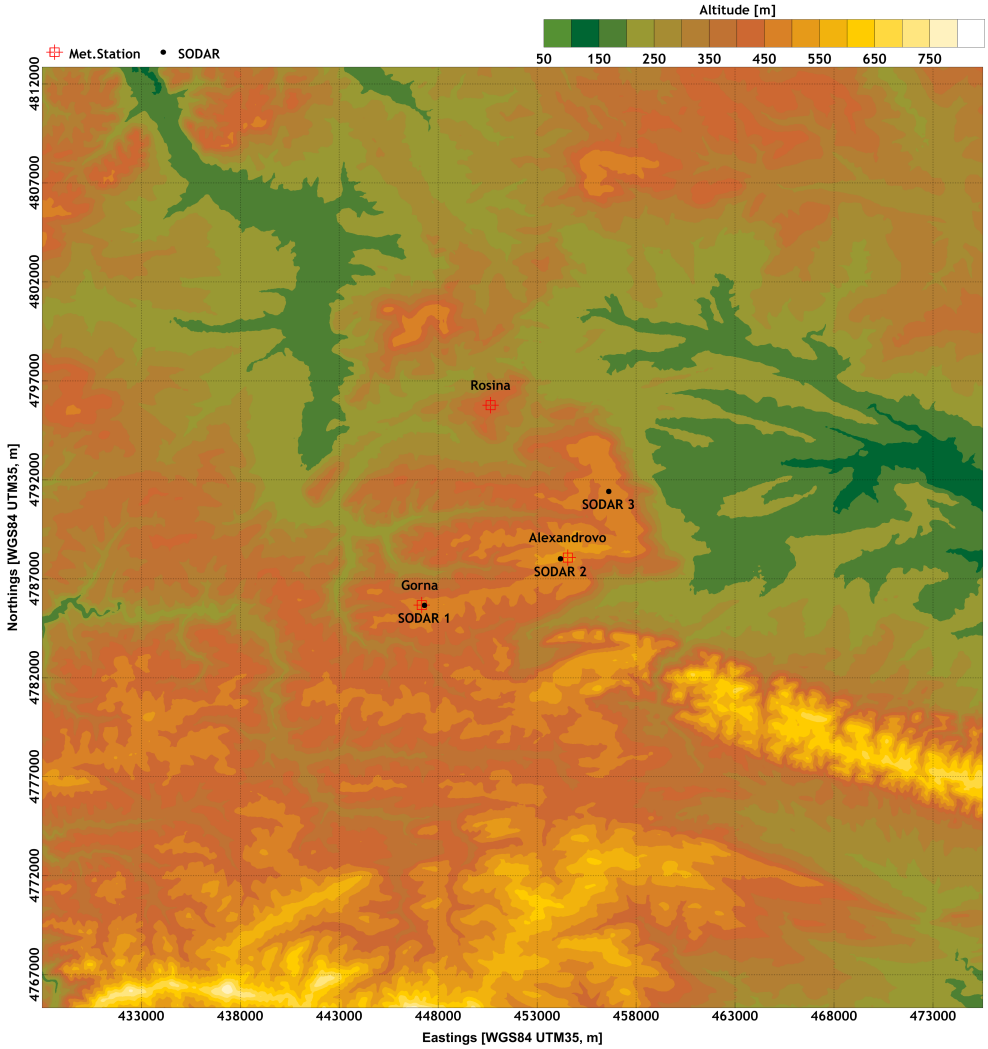

Figure 4.3: Topography map with the locations of the measuring points

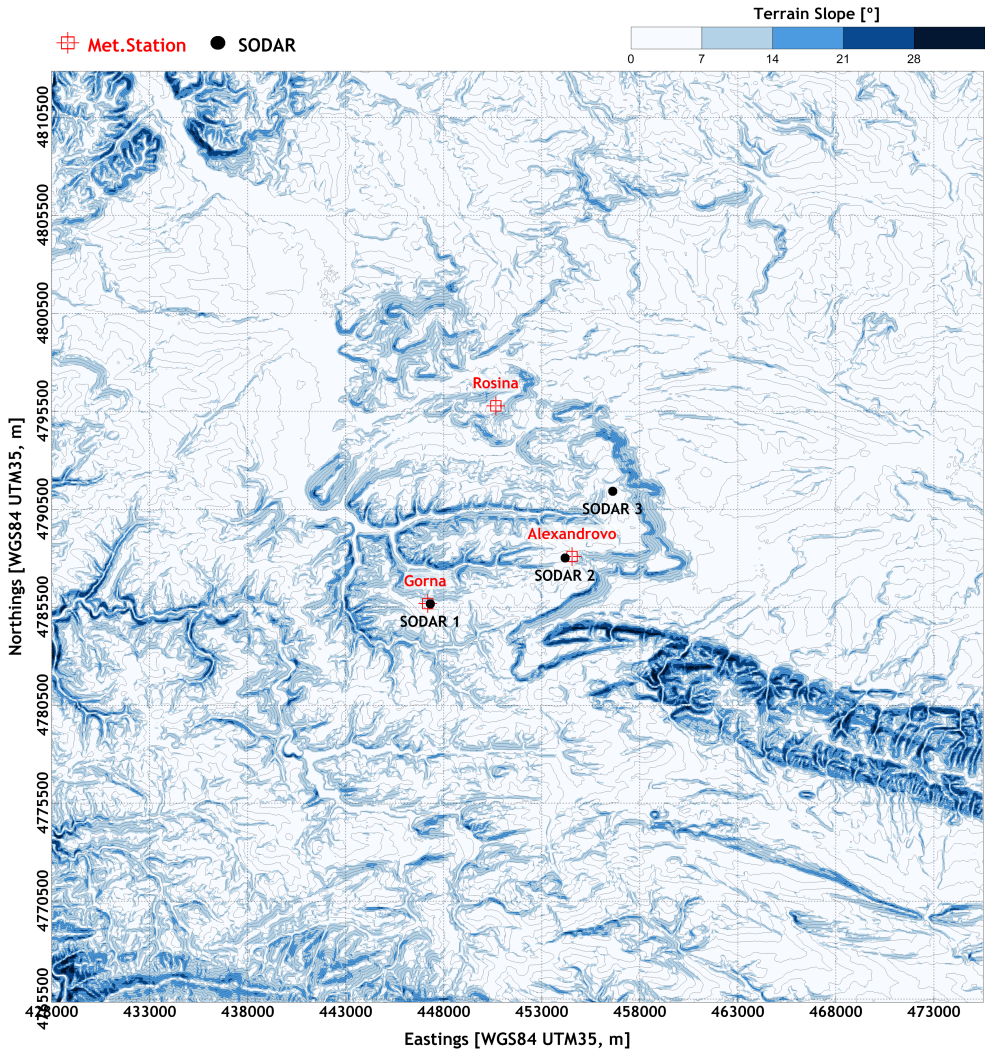

Figure 4.4: Terrain slope map

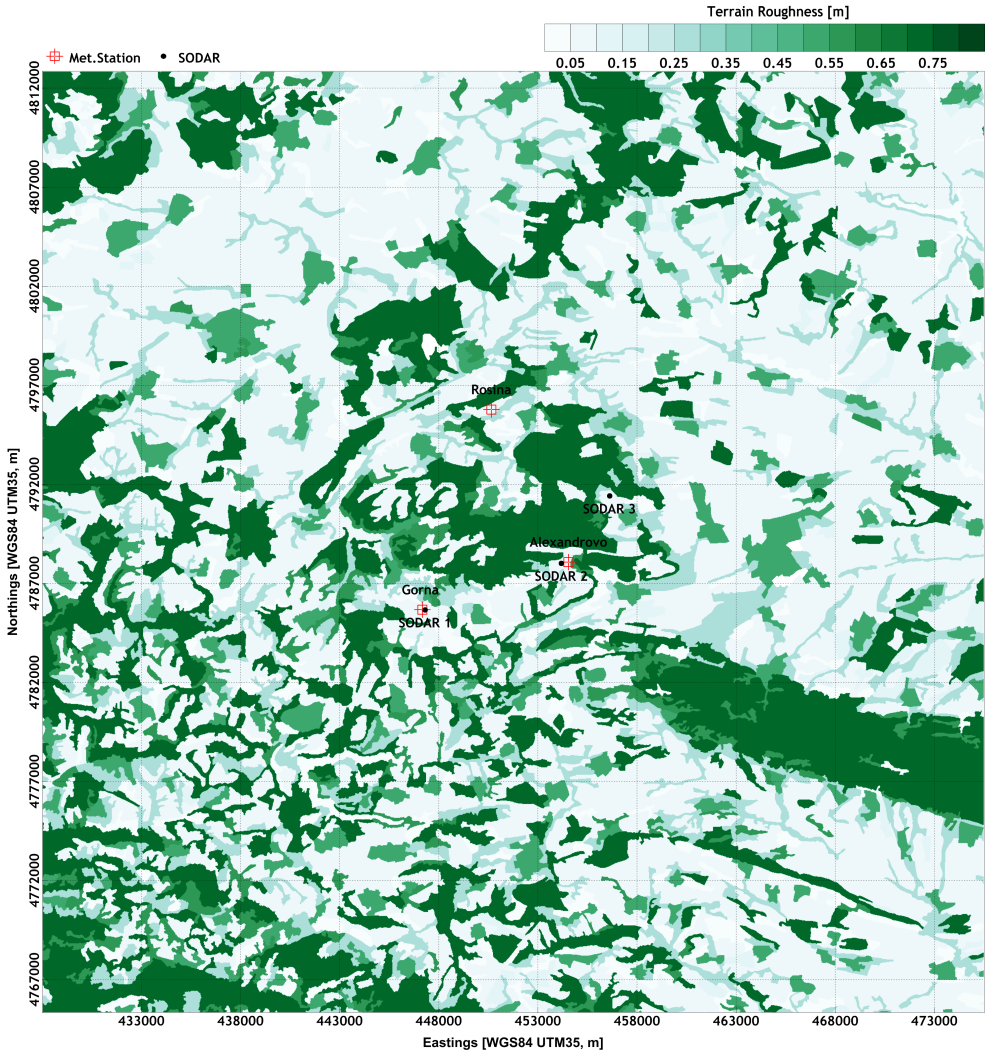

Figure 4.5: Terrain roughness map

4.2.3 Canopy forests description

The forest patches that surround the wind farm are composed by deciduous beech trees, or similar. The average tree height, according to MJ local assessment, is between 6 m and 20 m.

The MJ team defined three types of canopy forests:

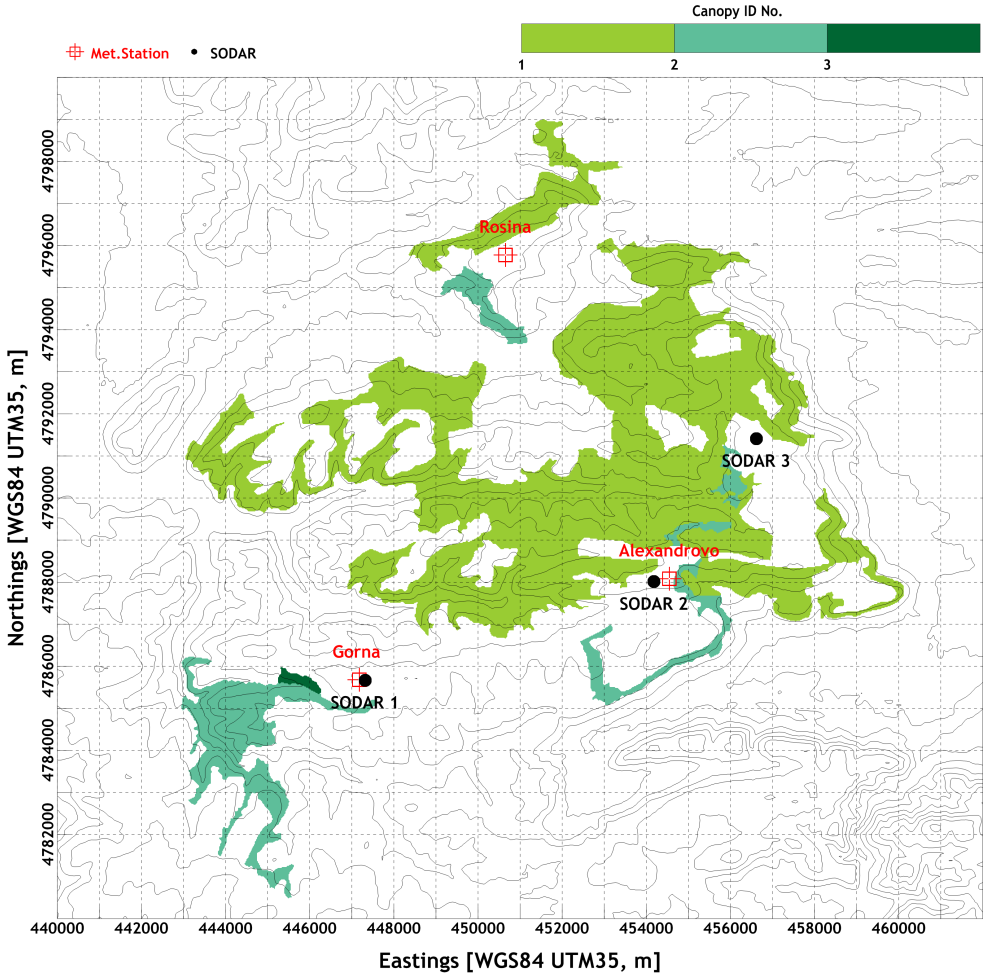

Figure 4.6: A-WF forest canopies map

In order to be able to use the abacus, the distances between the masts and the nearest upstream forest were measured for each wind direction.

The distances from forests to measure points are:

Direction	ALX 2	S3	ALX 3 - S2	ALX 1 - S1
0	325 (1)	450 (1)	770 (1)	2100 (1)
30	570 (1)	280 (1)	1000 (1)	2150 (1)
60	2400 (1)	285 (1)	170 (2)	3000 (1)
90	2650 (1)	390 (1)	120 (2)	5500 (2)
120	2300 (1)	-	265 (2)	-
150	2300 (1)	3100 (1)	1825 (2)	150 (2)
180	1500 (2)	2120 (1)	1950 (2)	600 (2)
210	700 (2)	875 (2)	2900 (2)	700 (2)
240	825 (1)	550 (2)	-	950 (2)
270	1350 (1)	700 (1)	1000 (1)	1150 (3)
300	350 (1)	750 (1)	400 (1)	-
330	285 (1)	610 (1)	-	4600 (1)

Table 4.1: Distances of forest canopies

4.3 Real wind data measurement

Three Mast and three Sodar were available. The following tables describe the major characteristics of Masts and SODAR measurement sites.

4.3.1 Measurement equipment location

The coordinates of the measurement equipment are:

	Coordinates WGS84 UTM35	
Measure Station	Eastings (m)	Northings (m)
Alexdrandovo	454546	4788082
Rosina	450652	4795776
Gorna	447176	4785676
SODAR 1	447316	4785665
SODAR 2	454183	4788013
SODAR 3	456617	4791411

Table 4.2: Coordinates of met masts and SODAR

4.3.2 Wind data analysis

For the wind data analysis, the following aspects have been considered:

- Different positions of measurement points.
- Coincident period of wind data extractions.
- Same height of wind measurements.

Therefore, the practise case situation according wind data of Gorna Kabda (ALX1), Rosina (ALX2), Alexandrovo (ALX3) and Momino (S3) have been studied.

The wind data analysis has been made from May to November in 2010 and 40 m a.g.l..

4.4 Simulation wind data analysis

The simulation has been made with software WINDIE^{TM} for all directions of the wind, with an increment of thirty degrees. The following table shows the simulation characteristics:

Direction	N	$COF_{X,Y,Z}$	Δ
i (x)	190	100	24000
j (y)	190	100	24000
k (z)	55	$h_c/10$	4500

Table 4.3: Mesh features in Alexandrovo, for 000°, 030°, 090°, 120°, 150°, 180°, 210°, 240°, 270°, 300°

Direction	N	$COF_{X,Y,Z}$	Δ
i (x)	190	80	20000
j (y)	190	80	20000
k (z)	55	$h_c/10$	4500

Table 4.4: Mesh features in Alexandrovo, for 060°, 330°

4.5 Comparations of wind data, Real VS Simulation

By making a comparison of the ratios of the real and simulated results, we can establish a trend in change of the h_c. According to the studied literature and parametric study, an increase in h_c represents a decrease of v_h and an increase of TI and SF.

4.5.1 Preliminary analysis

A first idea about how to modify the heights with the ratios of v_h, TI and SF in the positions where the measurement stations have been located, is explained in the following paragraphs.

Depending on the difference between the ratios of the real and the simulated values, the h_c has to be modified in the simulations so that the difference between simulated and the real values decreases as much as possible.

The concept then is to calculate the differences in simulated and real values of, say, TI, and use the abacuses to get an estimate of the required value of h_c to obtain a better agreement with measurements.

Considering the conclusion obtained in the previous Chapter: for modifications of α there is no significant variation of v_h, TI and SF. So, only adjustments to the forest canopy height will be sought here.

Consider the following example, where for 0°winds it was observed that:

$$\left(\frac{v_{ALX1}}{v_{ALX3}}\right)_{SIMU} > \left(\frac{v_{ALX1}}{v_{ALX3}}\right)_{REAL} \tag{4.1}$$

As ALX1 is more distant from the canopy ID1 than ALX3, (see table 4.1), ALX3 should be influenced by the forest. To improve agreement and minimise the above inequality, we would like to increase $v_{ALX3_{SIMU}}$ with respect to $v_{ALX1_{SIMU}}$.

It follows that we should try to reduce the impact of the forest in this case and therefore the value of h_c of canopy ID1 should decrease.

Similar analyses can be carried out for all the masts and considering TI and SF.

The following table lists the conclusions expressed by the analysis of the results described in the preceding paragraph, for all the ratios in which the relative difference between simulated and real values are greater than 20%.

Please note that TI measurements were not considered for the SODAR due to the inaccuracy of these type of instruments when measuring TI.

Canopy ID	v_h	TI	SF	Final
1	down	down	is not clear	down
2	up	down	is not clear	up
3	do not change	down	down	down

Table 4.5: Height changes

In the study of h_c according to the SF we attempted to obtain the value of this at 40 m for all points of measurements, but it was not possible for all points and it has been instead obtained ar nearby heights.

	ALX1	ALX2	ALX3	S3
$z_{v_h 1}$	60	49.5	58	50
$z_{v_h 2}$	20	40	20	40
z_{sf}	40	44.75	39	45

Table 4.6: Heights used for to obtain the SF

According to this preliminary analysis of results and as a consequence of the contradictions it can be stated that the distributions of canopy ID1 and ID2 should be modified and treated separately.

The distances to the forest canopy border are shown in the following table 4.7. These will be used as input to the abacuses. Having analysed the upstream topography slope in each case, we have indentified the appropiated abacus to use in each case listed.

Wind direction	Measurement stations	Distances of forest border, $x(m)$	Abacus used
0°	ALX2	325	Flat
60°	ALX3	170	+14°
90°	ALX3	120	+14°
240°	ALX1	950	Flat
270°	ALX1	1150	Flat

Table 4.7: Distances after to canopy border

4.5.2 Applying the Abacus Results

In this section, the values of h_c, using the abacus generated in the parametric study, are confirmed and quantified. The abacus for flat terrain is considered, because the real terrain is represented better in this case.

Before proceeding, we will identify the most relevant wind directions based on the measured wind roses below. To limit range of the analysis we will focus on the prevalent directions of: 0°, 60°, 90°, 240°and 270°.

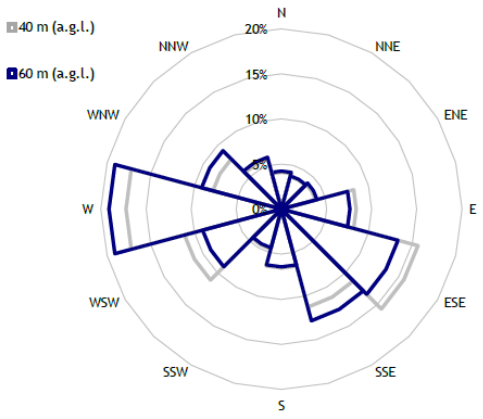

Figure 4.7: Frequency Wind Rose, ALX1

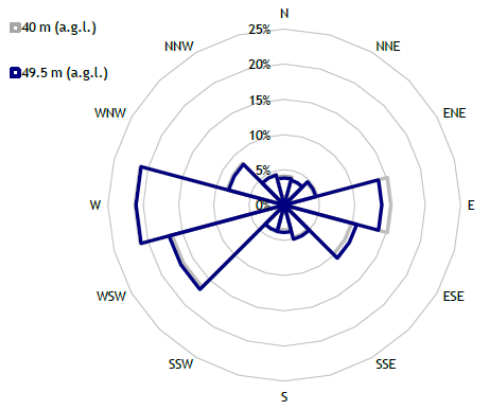

Figure 4.8: Frequency Wind Rose, ALX2

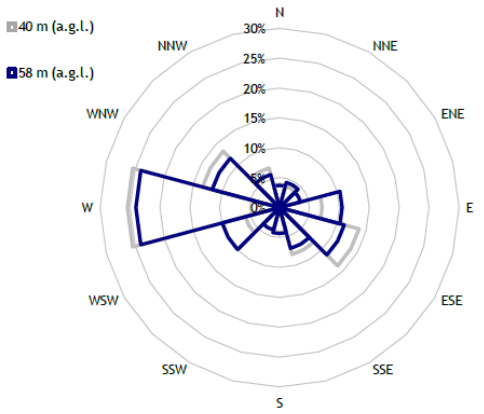

Figure 4.9: Frequency Wind Rose, ALX3

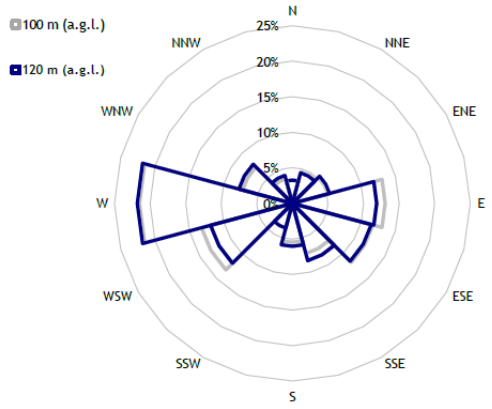

Figure 4.10: Frequency Wind Rose, S3

To isolate the effects of each forest pach as much as possible, we performed three sets of cases; with different reference masts:

- For 0°, we foussed on the northern area of Rosina (reference mast ALX2) considering canopy ID1 and ID2 of the same h_c.
- For 60°and 90°, the area of Alexandrovo (reference mast ALX3) considering canopy ID1 and ID2 of the same h_c.
- For 240°and 270 °, the area of Gorna (reference mast ALX1) considering canopy ID2 and ID3 of the same h_c.

Example. Wind: 0°, Area: Rosina, Reference Mast: ALX2, Canopy area: ID1.

The process for working with the abacus is as follows:

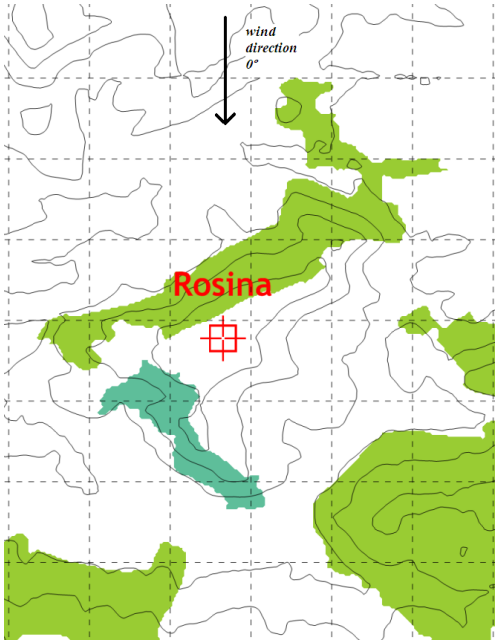

Figure 4.11: Zoom on Rosina area

We calculate the difference between the values of TI (and SF) real and simulated:

$$\Delta ti = ti_{real} - ti_{simu} = +5.75\% \tag{4.2}$$

$$\Delta sf = sf_{real} - sf_{simu} = +0.0842 \tag{4.3}$$

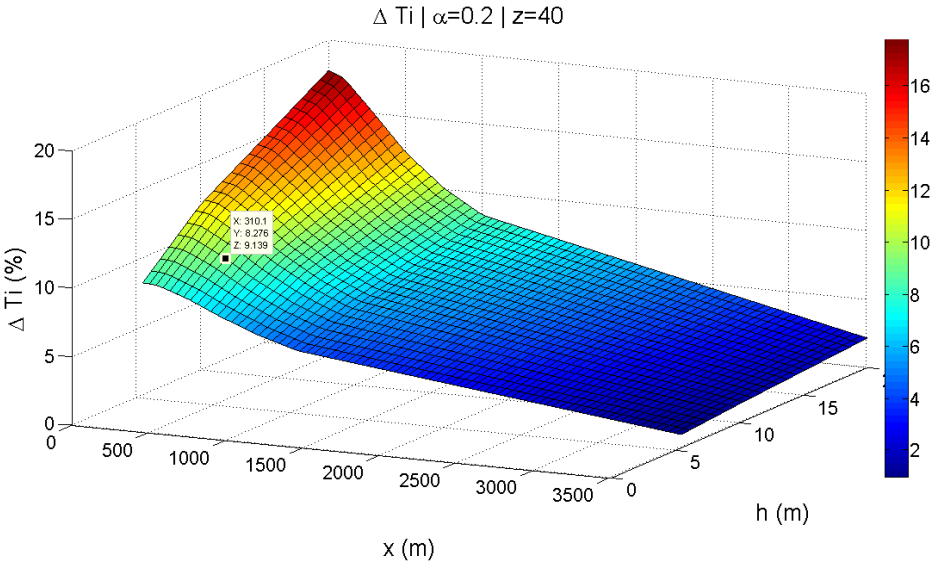

Figure 4.12: TI for 0°, plain terrain abacus

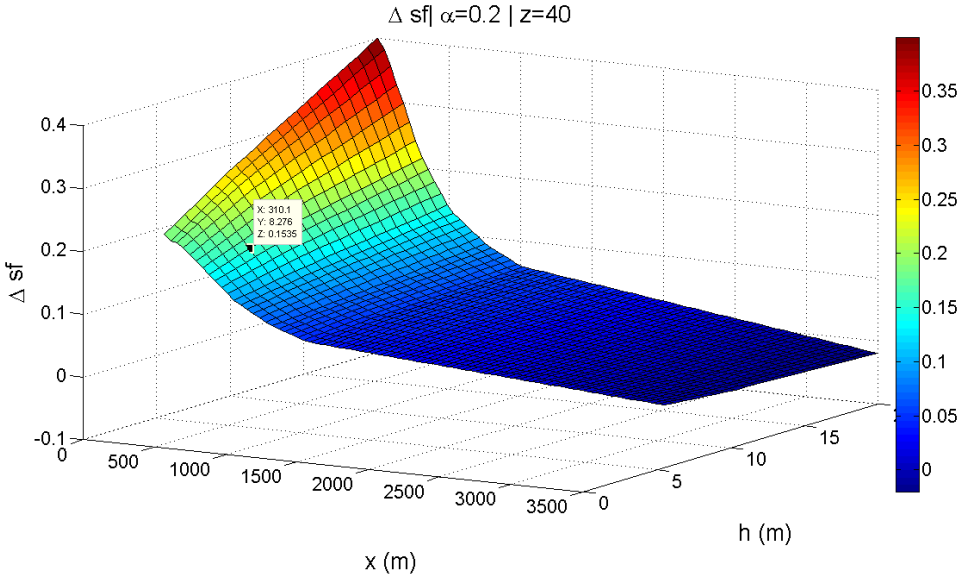

Figure 4.13: SF for 0°, plain terrain abacus

Knowing that the initial guess for the height of ID1 was $h_c = 8\,\mathrm{m}$, we check the abacus, to observe that:

$$ti(h = 8\,m) = 9.4\% \tag{4.4}$$

However, we are seeking a measured value of:

$$ti'(h = ?) = 9.14\% + 5.75\% = 14.89\% \tag{4.5}$$

This corresponds to a height according to the abacus of h_c=20 m.

Proceeding in the same way for the SF:

$$sf(h = 8\,m) = 0.15 \tag{4.6}$$

The SF is:

$$sf'(h = ?) = 0.15 + 0.0842 = 0.2342 \tag{4.7}$$

And corresponds to a height dependent on the abacus of h_c=20 m.

We conclude that for the next iteration to the canopy ID1 and ID2 will be h_c=20 m.

Applying the same procedure to the other wind directions and to each area we obtained the new estimates of forest heights based on TI (table 4.8), SF (table 4.9) and the forest heights chosen (table 4.10).

Direction	Canopy ID1	Canopy ID2	Canopy ID3	$h_c(m)$
0°	X	X		20
60°	X	X		7
90°	X	X		9
240°		X	X	5
270°		X	X	5

Table 4.8: h_c based on TI

Direction	Canopy ID1	Canopy ID2	Canopy ID3	$h_c(m)$
0°	X	X		20
60°	X	X		9
90°	X	X		11
240°		X	X	20
270°		X	X	7

Table 4.9: h_c based on SF

Direction	Canopy ID1	Canopy ID2	Canopy ID3	$h_c(m)$
0°	X	X		20
60°	X	X		7
90°	X	X		10
240°		X	X	20
240°		X	X	5
270°		X	X	5

Table 4.10: h_c for final simulation

Two facts stand out from the previous tables:

- The values of h_c vary significantly for 0°, 60°and 90°. This strongly suggests that the northern patch at Rosina and the large central forest should be treated separately.

- Significantly different calues of h_c were obtained for 240°and 270°, depending on whether the TI or SF abacus we used.

4.6 Simulations with updated forest heights

Acording of the abacus, forest heights should be changed as listed before. Six additional simulations were carried out to evaluate performance of the procedure.

We will now analyse the effects of the changes in h_c.

0°- ALX2	TI	SF	Cano ID1	Cano ID2	Cano ID3
			h_c (m)		
Initial simulation	0.1119	0.15	8	10	12
Final simulation	0.1288	0.23	20	20	12
Real measurement	0.1695	0.2342	-	-	-

Table 4.11: Values of TI and SF for 0°

60°- ALX3	TI	SF	Cano ID1	Cano ID2	Cano ID3
			h_c (m)		
Initial simulation	0.1909	0.29	8	10	12
Final simulation	0.1799	0.27	7	7	12
Real measurement	0.1728	0.2595	-	-	-

Table 4.12: Values of TI and SF for 60°

90°- ALX3	TI	SF	Cano ID1	Cano ID2	Cano ID3
			h_c (m)		
Initial simulation	0.1775	0.28	8	10	12
Final simulation	0.1869	0.28	10	10	12
Real measurement	0.1597	0.3417	-	-	-

Table 4.13: Values of TI and SF for 90°

240°- ALX1 (a)	TI	SF	Cano ID1	Cano ID2	Cano ID3
			h_c (m)		
Initial simulation	0.1285	0.13	8	10	12
Final simulation	0.1382	0.14	8	20	20
Real measurement	0.1078	0.2239	-	-	-

Table 4.14: Values of TI and SF for 240°(a)

240°- ALX1 (b)	TI	SF	Cano ID1	Cano ID2	Cano ID3
			h_c (m)		
Initial simulation	0.1285	0.13	8	10	12
Final simulation	0.123	0.24	8	5	5
Real measurement	0.1078	0.2239	-	-	-

Table 4.15: Values of TI and SF for 240°(b)

270°- ALX1	TI	SF	Cano ID1	Cano ID2	Cano ID3
			h_c (m)		
Initial simulation	0.1551	0.18	8	10	12
Final simulation	0.1397	0.17	8	5	5
Real measurement	0.1177	0.1742	-	-	-

Table 4.16: Values of TI and SF for 270°

Wind result analysis.

For 0°. Whilst there has seen a marked improvement in SF, the increase in h_c has not increased TI sufficiently.

For 60°. A better agreemnet was obtained for TI, although the change in SF was insufficient.

For 90°. The slight increase in the height of canopy ID1 produced a slight increase in turbulence but a large increase in SF. In this instance the initial forest configuration produced better results, these results further suggest that other complex phenomena, other than the forest are affecting results.

For 240° wind direction and the option (a). The increase in the height of canopy ID2 and ID3 produced a slight increase in shear, which is insufficient.

For 240° wind direction and the option (b). The slight decrease in the height of canopy ID2 and ID3 produced a slight decrease in turbulence but a large increase in SF.

For 270° wind direction. The slight decrease in the height of canopy ID2 and ID3 produced a slight decrease in turbulence and SF.

4.7 Conclusions

As previously mentioned, we can conclude that the patches of canopy ID1 and ID2 should be modified and treated in a separate way, especially in ALX3 ans S3 areas with respect to the ALX2 met mast (area Rosina).

When a predominance of terrain against the canopy occurs produced, to extract reliable information of abacus for determine the h_c is difficult. The application of these abacuses in real terrain should therefore be done with care and results should be compared with measurements whenever possible.

Chapter 5

Conclusions and future work

5.1 Conclusions

In the present work, the effect of forests on the wind flow were studied. A method for predicting the forest characteristics has been developed, when we only have information about the distribution forests and the distances of measurement points to the beginning of the canopy.

The approoach consisted in building an abacus which could provide useful information about the effects of forests on the wind flow in terms of the v_h, TI and SF.

We have found difficulties in applying the abacus to the case study A-WF. There are, for the case of Alexandrovo, clear influences of terrain on wind flow, versus the effect caused by the forest.

However this should not be generalized, because in other areas where the degree of complexity is not as high as Alexandrovo, the abacus can be applied, and it can be studied according to the general situations that were established in the parametric study.

Must be establish the similarities between the terrain on parametric analysis and real case for that the level of validity is high.

As this coincidence is difficult to occur, we can make approximations of h_c, always taken as reference value and never as an exact value.

This is the main limitation that occurs in parametric study, and therefore also limits in the degree of applicability of the abacus.

It concludes that for areas with a lower complexity level the abacus should provide quantitative guidance to help define tree heights.

Therefore the most important conclusions are:

- The influences of α are negligible for wind flow behaviour.
- The abacus is not feasible for complex terrain, except as a rough qualitative guide.

5.2 Future work

The future work may be directed in four different aspects:

1. Applying the abacuses to a real case with truly flat forested terrain.
2. Deducting the terrain effects from wind flow and analyse only the forest effects. Increasing the simulation number without forest.
3. Making other parametric studies based on different configurations of terrain, doing a combination of mathematical function that describes our study area: sinusoid, impulse function, etc.

Bibliography

J. C. Kaimal and J. J. Finnigan. *Atmospheric boundary layer flows. Their structure and measurement*. Oxford University Press, 1994.

G. G. Katul, L. Mahrt, D. Poggi, and C. Sanz. One- and two-equation models for canopy turbulence. *Boundary-Layer Meteorology*, 113:81–109, 2004.

J. C. Lopes da Costa, F. A. Castro, J. M. L. M. Palma, and P. Stuart. Computer simulation of atmospheric flows over real forests for wind energy resource evaluation. *Journal of Wind Engineering and Industrial Aerodynamics*, 94:603–620, 2006.

R. N. Meroney. Characteristics of wind and turbulence in and above model forests. *Journal of Applied Meteorology*, 7:780–788, 1968.

D. E. Neff and R. N. Meroney. Wind-tunnel modeling of hill and vegetation influence on wind power availability. *Journal of Wind Engineering and Industrial Aerodynamics*, 74-76:335–343, 1998.

E. G. Patton. *Large-Eddy Simulation of turbulence flow above and within a plant canopy*. PhD thesis, University of California at Davis, U.S.A., 1991.

H. S. Pedersen and W. Langreder. Forest - added turbulence: A parametric study on turbulence intensity in and around forests. Technical report, Journal of Physics. Conference Series: no. 75., 2007.

M. R. Raupach, J. J. Finngan, and Y. Brunet. Coherent eddies and turbulence in vegetation canopies: the mixing-layer analogy. Technical report, CSIRO Centre for Enviromental Mechanics, Canberra, Australia, 1996.

J. Sanz Rodrigo, J. van Beeck, and G. Dezsö-Weidinger. Wind tunnel simulation of the wind conitions inside bidimensional forest clear-cuts. application to wind turbine siting. *Journal of Wind Engineering and Industrial Aerodynamics*, 95:609–634, 2007.

R. Shaw and U. Shumann. Large - Eddy simulation of turbulent flow above and within a forest. *Boundary-Layer Meteorology*, 61:47–64, 1992.

U. Svensson and K. Häggkvist. A two-equation turbulence model for canopy flows. *Journal of Wind Engneering and Industrial Aerodynamics*, 35:201–211, 1990.